JOURNAL OF COMPUTATIONAL PHYSICS **126,** 251–273 (1996)
ARTICLE NO. 0136

Explicit Generation of Orthogonal Grids for Ocean Models

ROSS J. MURRAY

School of Earth Sciences, University of Melbourne, Parkville, 3052, Victoria, Australia

Received January 5, 1995; revised October 11, 1995

Several explicit methods are proposed for generating global orthogonal curvilinear grids for ocean modelling. The methods are based on the conformal properties of stereographic and Mercator map projections and have been developed with the specific object of removing the North Pole from the ocean domain. Some of the configurations, in addition to overcoming the pole problem, have very attractive resolution properties in the polar regions. Two of the constructions are geometrical in nature, while a third is based on the superposition of potential fields generated by discrete coordinate poles. The methods described here differ from those commonly employed in engineering problems in that grid line control is exercised by the placement of a finite number of singularities, and no specific condition is placed upon the fitting of coordinate lines to physical boundaries. The grids produced are accordingly of global construction and have smooth variations in grid size. Being of analytical or semi-analytical formulation, the grids may be generated quickly and without the need for advanced software.

1. INTRODUCTION

The convergence of meridians at the North Pole has been a source of numerical difficulties in ocean modelling that have never been satisfactorily resolved. Many ocean modellers have simply avoided the problem by excluding the north polar region from their integrations altogether. When it has been included, it has been customary to apply Fourier filtering, which introduces a spurious and nonlocal forcing to the solutions. Another problem is that with staggered grids it is not possible to utilise a periodic boundary condition across the North Pole without having a line of grid points at the Pole itself, which creates a need for a special treatment of the polar point. Williamson [22] has discussed how this could be done, but the idea has never been applied to ocean models. Instead, it has been normal to specify a row of inactive points at the northernmost grid latitude, thus effectively creating a small island at the Pole, which in coarse resolution models must necessarily disrupt the transpolar circulation. In coupled ice–ocean models the presence of a polar island would also tend to distort the pattern of sea ice drift and hence of deep convection in the Greenland and adjacent seas. Even with a special treatment of the polar point, the strong curvilinearity of the parallels and the excessive number of poorly distributed latitude–longitude points would continue to cause difficulties.

Several authors have attempted to overcome the convergence problem by moving the poles of the spherical grid away from the area of interest. For modelling the Arctic Ocean, Semtner [16] used a rotated spherical grid with north and south poles lying on the Equator at 125°E and 55°W; the same rotation of the ocean grid has since been used in coupled ice–ocean models of the Arctic by Hibler and Bryan [8] and by Semtner [17]. Owing to the absence of land antipodes, which account for only $\frac{1}{10}$ of the world's land area and nowhere lie sufficiently far inland to overcome the need for filtering (see Fig. 1), the expedient of a simple rotation cannot be used for a global ocean grid. To obviate this difficulty, Deleersnijder *et al.* [4] and Eby and Holloway [5] have proposed a coordinate system in which the North Atlantic and Arctic Oceans are represented by a spherical grid rotated through an angle of 90° so as to remove the poles from the computational domain; the rotated grid is joined along the Equator in the Atlantic Ocean to a conventional latitude–longitude grid, which is used to model the remaining four-fifths of the world ocean. The scheme has the advantage of requiring for its implementation only minor changes to the coding of some commonly used models (such as the Cox–Bryan model): its drawbacks are that (a) the poles of the rotated grid are fixed in latitude and longitude by the requirements of matching the grids in the equatorial Atlantic, (b) the matching tends to impose a pattern of zonal resolution which may not be optimal at high northern latitudes, (c) there is a small discontinuity of grid size across the connection line, and (d) the subgrids cannot be matched across the Bering Strait.

Having somewhat exhausted the possibilities of using spherical coordinates, it is logical to consider whether curvilinear coordinates might be employed. Numerical methods have been developed for generating curvilinear computational grids for a variety of engineering applications, often involving problems of aerofoil and channel flow. In such problems, keeping boundary separation to a minimum is normally an implicit requirement, and it makes good sense to align the coordinates with the physical boundaries and expected flow lines. The emphasis has therefore been

0021-9991/96 $18.00

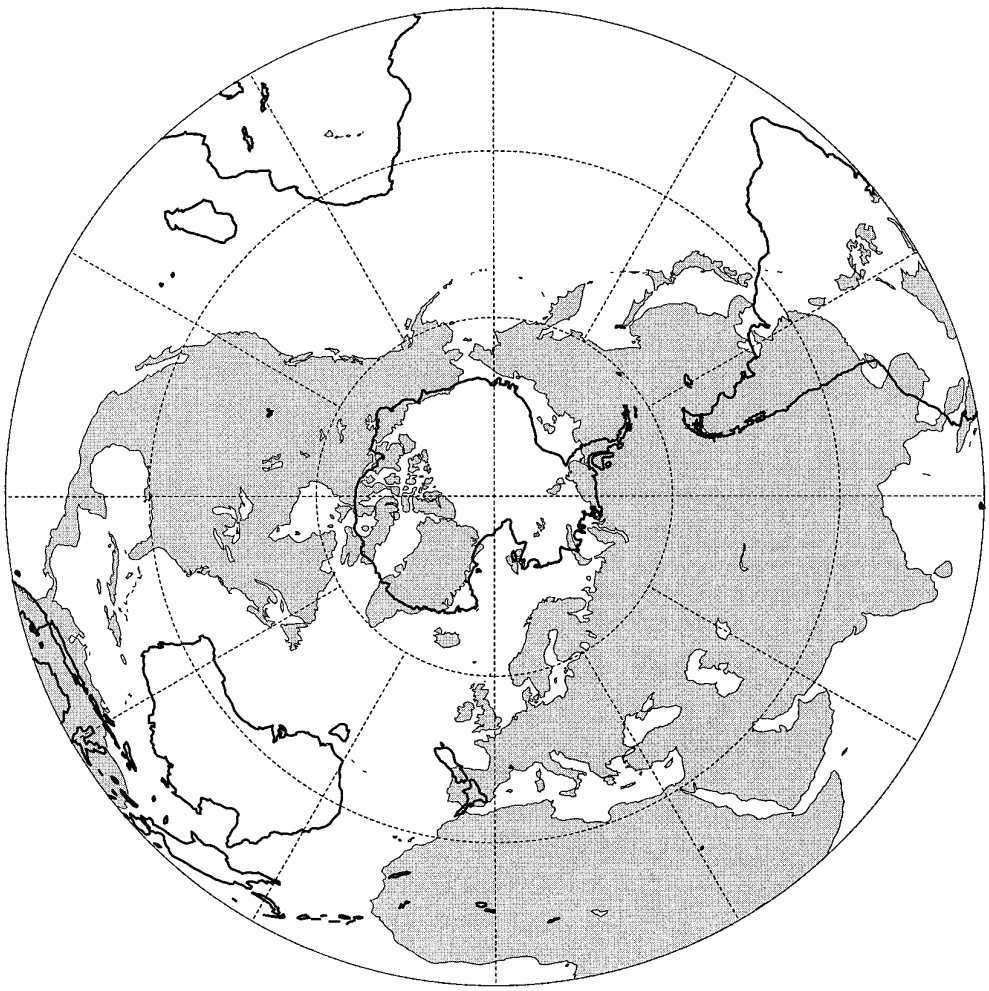

FIG. 1. Map of the Antipodes (azimuthal equal area projection). Land areas in the NH are shown stippled and in the SH (reversed) with bold outlines.

on boundary-fitted coordinate systems. A review of boundary-fitted grid generation techniques is given by Thompson *et al*. [19]. In the type of method most commonly used, the grid is obtained as the solution of an elliptic boundary value problem; the solution of Laplace's equation, in particular, results in a conformal grid. Conformal grids are automatically orthogonal and have a very smooth distribution of interior points.

In the last few years, numerical grid generation methods have also begun to be used in ocean modelling. Wilkin [21] has adapted the conformal grid generation techniques of Ives and Zacharias [9], and curvilinear grids generated by his program have been used in connection with the semi-spectral primitive equation model (SPEM) of Haidvogel *et al*. [6] and the coastal ocean numerical model of Blumberg and Mellor [1]. The grid package allows the operator to specify the geographical alignments of four boundary segments (corresponding to the sides of the rectangular grid array) and the spacing of points along two of the sides. One or more of the coordinate boundaries can usually be made to conform to a spline-smoothed coastline.

While coast-following boundaries may be desirable for some regional applications, the rationale for using boundary-fitting techniques to generate global ocean grids is less compelling. The world's oceans have irregular coastlines which cannot ordinarily be followed conveniently; indeed, it may be in the interests of numerical stability *not* to adapt the bounding coordinates to coastlines too rigorously, as grid spacing can become very small near convex boundaries and is difficult to control in sinuous ocean basins. There are properties that are of greater value in a global ocean grid; the chief of these would be the following:

1. *Orthogonality*. Grids used for modelling hydrodynamic flows are not always orthogonal, but departures from orthogonality require the computation of extra terms in

the model equations. For efficiency and accuracy in long-term integrations this property is highly desirable.

2. *A slow variation of grid spacing along grid lines.* The accurate estimation of spatial derivatives using centred finite differences demands that the variation in grid intervals from point to point should be as gradual as possible; this property is likely to be violated when grid compression is applied roughly or when differently constructed subgrids are joined in a composite fashion.

3. *A moderate overall range of grid spacing.* Because of the restriction which the minimum grid spacing places on the maximum permissible time step, a wide variation of grid size makes for an inefficient use of computational resources. Furthermore, large grid size variations and the high aspect ratios (elongated cells) that often accompany them are wasteful of spatial resolution unless these characteristics have been specifically designed to reflect corresponding variations in the expected structure of the solution.

4. *An absence of singular behaviour over the ocean.* A singularity not only creates a ''dead'' area and all the problems associated with very small grid size (including the need for filtering), but also it generates strong grid line convergence and curvilinearity in the area around it. Convergence results in a *transverse* variation in grid size, even though the grid may be equidistant or have little variation *longitudinally.* The finite difference operators in the model do contain factors which allow for this variation, but the allowance may be insufficiently accurate when the variation is rapid, as is the case close to singularities.

Other features which may be of greater or lesser importance, depending on the application, are discussed where relevant. These might include a closer spacing or preferred alignment of grid lines in particular regions, an ability to represent the world ocean on a single rectangular lattice, or a requirement for global continuity of grid lines by the use of reentrant boundary conditions.

Numerical grid generation methods, and in particular conformal methods, are quite capable of producing orthogonality and regularity, but impose severe limitations to the control which the designer can exercise over the alignment and spacing of grid lines. Also, they normally require advanced software and, because of constraints on boundary matching, have not yet been adapted to mapping multiply-connected regions on the sphere. In this article, a quite different approach is taken. It is shown that a number of orthogonal curvilinear coordinate systems can be constructed quite simply by analytical means, using the properties of conformal map projections. In their basic form, the grids are global and have no discontinuities of grid size; but, even when composite constructions are used, such discontinuities can be suppressed. The grids have been specifically designed to remove the north polar singularity from the ocean domain. Three different approaches have been taken to accomplish this: in Section 2, a geometric transformation is used to effect an asymmetrical placement of the north and south grid poles (the asymmetrical bipolar grid); in Section 3, a coodinate system composed of confocal ellipses and hyperbolae is derived (the confocal grid); and in Section 4, it is shown that grids can be generated about an arbitrary number of poles, using a formulation based on concepts borrowed from electrostatic theory (the multipolar grid).

A global coordinate system which is curvilinear but not boundary-fitted has been developed at the Laboratoire d'Océanographie Dynamique et de Climatologie (LODYC) and is described by Madec and Imbard [11]; it consists of a Southern Hemisphere (SH) latitude–longitude grid joined to a curvilinear Northern Hemisphere (NH) grid in which the north grid pole has been moved into northern China. On a polar stereographic projection, the mesh consists of a family of embedded circles whose centres are positioned along a chosen meridian of longitude according to a formula and another family of curves which is constructed to meet them at right angles using a second-order finite difference integration of a differential equation. The NH part of the mesh is strikingly similar to the asymmetrical grid developed in Section 2, but it is not based on a geometrical construction; rather, the procedure is one which the authors appropriately categorise as ''semi-analytical'' and which is related to the method recommended in the Appendix for merging the elements of a rotated grid. In this respect it complements the scheme of global coordinate constructions that emerges from this article.

2. ASYMMETRICAL BIPOLAR GRIDS

2.1. *Grids Constructed by Reprojection*

The difficulty of finding suitable locations for the coordinate poles over land is one that can be overcome by applying a transformation which contracts the coordinate lines towards one side of the globe and expands them away from the other, thus placing the poles in an off-diagonal alignment. Geometrically, this is accomplished by stereographically projecting the latitude-longitude coordinates of one sphere (the grid sphere) onto a tangent plane and then *reprojecting* them onto a second sphere of different radius (the true sphere). Since each of these transformations is conformal, the resultant transformation will be so too, and the transformed grid will be orthogonal. Also, because of the nature of the projection, all of the transformed grid lines will remain circular. Figure 2 shows an example of a spherical grid remapped by this type of operation. Combined with an appropriate rotation, the projection-reprojection transformation can be used to place the poles of the grid at any two chosen locations on the Earth.

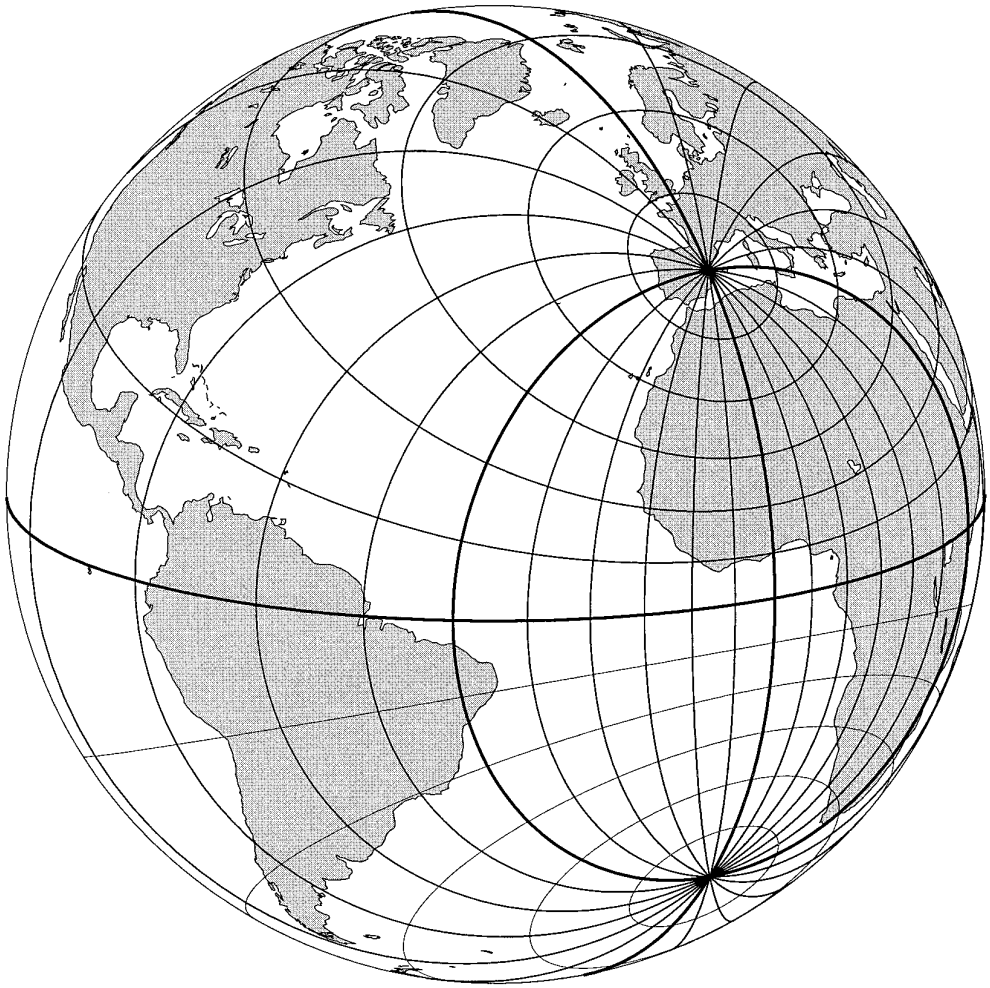

FIG. 2. A 15° × 15° spherical grid reprojected about the point 0°N, 0°E, with grid poles at 40°N and S, 0°E (oblique orthographic projection). The Equator and Greenwich meridian (bold lines) remain in their usual positions, but the 90° meridian and "near hemisphere" enclosed by it have been contracted toward the tangent point.

In their basic orientation, the two spheres have axes parallel to each other and to the projection plane, upon which they are cotangent. The construction is shown on the left side of Fig. 3, and to the right of it is a plan view of part of the projection plane. The combined effect of projection and reprojection is essentially a remapping of the angular distance χ_c, of any point X from Q on the grid sphere (the *curvilinear* coordinate system), to χ_s, on the true sphere (the *spherical* coordinate system). The azimuthal angle, θ, of QX with respect to the prime meridian is unchanged in this operation; nevertheless, it will be separately defined as θ_c for the grid sphere and θ_s for the true sphere, to allow for the possibility of rotation. Upon reprojection, the poles of the curvilinear grid (P_1 and P_2) are displaced equal distances toward the Equator (Q), their angular separation from it being reduced from 90° to χ_P. The radial distances, r and r_P, of X and P_1 from Q can be given in terms of these angles by

$$r = r_P \tan(\chi_c/2) = r_N \tan(\chi_s/2),$$
$$r_P = r_P \tan(90°/2) = r_N \tan(\chi_P/2).$$

To simplify the expressions, the projection is scaled to make r_N equal to unity. Dividing r by r_P and rearranging then yields

$$\tan\frac{\chi_s}{2} = r_P \tan\frac{\chi_c}{2}, \tag{1}$$

where

$$r_P = \tan(\chi_P/2). \tag{2}$$

The angles χ_c and θ_c are simply related by trigonometric relations to the longitude and latitude, λ_c and ϕ_c, of X on the grid sphere (Fig. 4a). In the standard case, χ_s

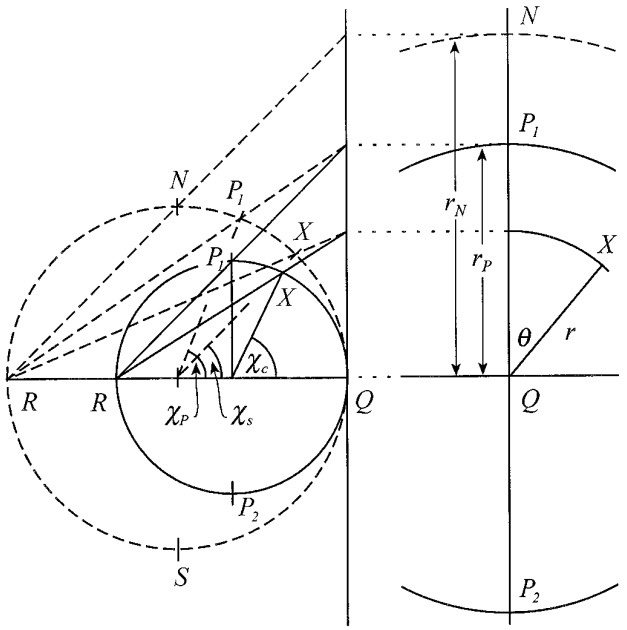

FIG. 3. Points on the grid sphere (solid circle) are stereographically projected onto a plane (shown in plan at right) and then reprojected onto the true or geographical sphere (dashed circle). Q is the tangent point (the pole of the projection), P_1 and P_2 are the "north" and "south" poles of the grid, N and S are the true N and S Poles, and X is a representative point; r, r_P, r_N are respectively the radial distances of X, P_1, and N from Q on the projection plane.

and θ_s are correspondingly related to λ_s and ϕ_s on the true sphere; however, since the grid poles will not normally be symmetrically placed with respect to the Equator, a sequence of Euler rotations is also necessary. These are defined by the coordinates (λ_Q, ϕ_Q) of Q and the bearing (β) of the prime grid meridian from the true north direction (Fig. 4b). For notational convenience, the complements of angles are indicated by primes (e.g., $\phi'_Q = 90° - \phi_Q$) and the spherical cosine and tangent functions are defined with reference to a spherical triangle having vertices (A, B, C) and opposite sides (a, b, c) by the formulae

$$a = f_c(A, b, c) = \cos^{-1}(\cos A \sin b \sin c + \cos b \cos c),$$
$$B = f_t(A, b, c) = \text{atan2}\,[\sin A, (\sin c/\tan b - \cos c \cos A)],$$

where atan2(x,y) is the FORTRAN "atan2" function, which gives the polar angle measured clockwise from the N direction of a point having cartesian coordinates (x, y). Using these definitions, one can write the following sequence of equations for obtaining the angles χ_P, λ_Q, ϕ'_Q, and β from the coordinates (λ_1, ϕ_1) and (λ_2, ϕ_2) of the grid poles P_1 and P_2:

$$\chi_P = \tfrac{1}{2} f_c(\lambda_1 - \lambda_2, \phi'_2, \phi'_1),$$
$$\alpha = f_t(\lambda_1 - \lambda_2, \phi'_2, \phi'_1),$$
$$\lambda_Q = \lambda_1 - f_t(\alpha, \chi_P, \phi'_1),$$
$$\phi'_Q = f_c(\alpha, \phi'_1, \chi_P),$$
$$\beta = f_t(\alpha, \phi'_1, \chi_P).$$

The distance, r_P, can then be obtained using Eq. (2). Having precalculated the parameters, λ_Q, ϕ'_Q, β, and r_P, the transformation for any point X can be carried out in the following steps:

1. transform (λ_c, ϕ_c) to (θ_c, χ_c),

$$\chi_c = f_c(\lambda_c, \phi'_c, 90°) = \cos^{-1}(\cos \lambda_c \cos \phi_c),$$
$$\theta_c = f_t(\lambda_c, \phi'_c, 90°) = \text{atan2}(\sin \lambda_c, \tan \phi_c);$$

2. transform χ_c to χ_s (Eq. 1);
3. rotate θ_c through an angle β, $\theta_s = \theta_c + \beta$;
4. transform (θ_s, χ_s) to (λ_s, ϕ_s),

$$\lambda_s = \lambda_Q + f_t(\theta_s, \chi_s, \phi'_Q),$$
$$\phi_s = 90° - f_c(\theta_s, \chi_s, \phi'_Q).$$

The local enlargement effected by the projection–reprojection, or reciprocal of the map factor m, is a function of χ_c alone and is given by differentiating Eq. (1),

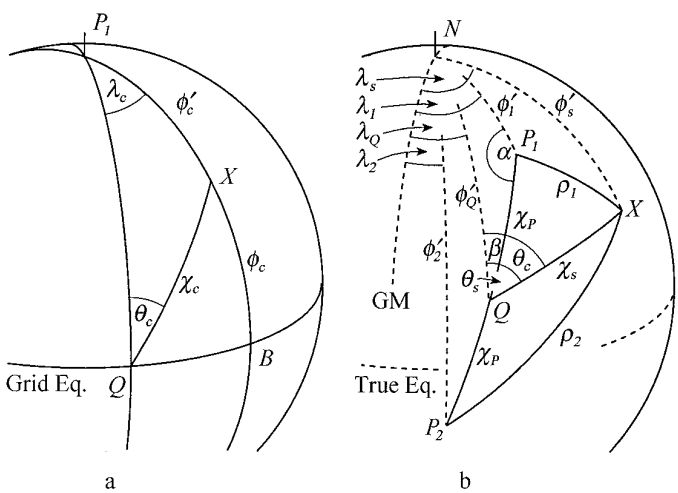

FIG. 4. Angles on the (a) grid sphere and (b) true sphere associated with the generation of a bipolar grid. GM denotes the Greenwich meridian.

$$\frac{1}{m} = \frac{\partial \chi_s}{\partial \chi_c} = r_P \frac{\sec^2(\chi_c/2)}{1 + r_P^2 \tan^2(\chi_c/2)}; \tag{3}$$

its value ranges between r_P at Q and $(1/r_P)$ at R.

The map factor enters into the expression for the metric coefficients, which are needed for calculating spatial derivatives in numerical models. A metric coefficient or factor (or scaling factor), $\partial s/\partial \sigma$ (or h_σ), is the distance, Δs, on the Earth corresponding to unit change in some grid-related coordinate, σ, such as latitude or longitude or other angular or projection plane coordinate (e.g., Williamson [22]; Deleersnijder *et al.* [4]). Alternatively, the coordinate may be a nondimensional array variable having integral values at grid points. In the latter case, the metric factors are just instantaneous estimates of the grid spacings (or their reciprocals, as in the usage of Haidvogel *et al.* [6]). For the bipolar grid, the analytical expressions for the metric coefficients, given as derivatives of λ_c and ϕ_c and of the array variables, $\xi = \lambda_c/\Delta\lambda_c$ and $\eta = \phi_c/\Delta\phi_c$, are

$$\begin{aligned} \frac{1}{\Delta\lambda_c}\frac{\partial s}{\partial \xi} &= \frac{\partial s}{\partial \lambda_c} = \frac{a \cos \phi_c}{m}, \\ \frac{1}{\Delta\phi_c}\frac{\partial s}{\partial \eta} &= \frac{\partial s}{\partial \phi_c} = \frac{a}{m}, \end{aligned} \tag{4}$$

where a is the radius of the Earth. The expressions are the same as for spherical coordinates except for the factor $1/m$.

To limit the variation of map factor as much as possible, the polar separation ($2\chi_P$) should be chosen to be fairly close to 180°. Three pairs near-antipodal land areas suggest themselves in Fig. 1: N Canada–E Antarctica, Siberia–W Antarctica, and China–Argentina. A coordinate grid with poles at (100°W, 65°N) and (80°E, 85°S) is shown in Fig. 5. In this example the poles are 160° apart, so the variation of $(1/m)$ is fairly modest (0.84 to 1.19). The positioning of the north pole over Canada has resulted in grid parallels which nicely follow the bend of the Arctic.

One desirable feature lacking in this type of configuration is that the grid equator does not run parallel to the Earth's equator; this may be a disadvantage when grid compression is contemplated for better simulating the equatorial circulation. It is not the orientation of the grid lines themselves that is necessarily the problem, but rather the inability of keeping a narrow concentration of grid lines within the equatorial zone. The grid can be *made* to coincide with the Earth's equator by using a composite construction in which the mesh for each hemisphere is separately generated from a symmetrical arrangement of poles. For the SH this would simply mean using the familiar spherical grid. The NH grid could be taken from the northern half of a global grid with poles located on the same meridian and at equal latitudes N and S. For continuity of the meridians at the Equator, the grid longitudes, λ_c, would need to be rechosen according to

$$\tan\frac{\lambda_c - \lambda_1}{2} = \frac{1}{r_P}\tan\frac{\lambda_s - \lambda_1}{2},$$

where the λ_s are the longitudes used in the SH. A composite grid with a north pole placed at 62°N, 101°W is illustrated in Fig. 6. It is clear that the combination has only partly succeeded in its objective. Owing to the smaller polar separation used in the composite arrangement ($2\chi_P = 124°$, as compared to 160° in Fig. 5), the variation of $1/m$ around the Equator is quite large (0.60 and 1.66). This means that at most longitudes there is quite a jump in grid size on crossing the Equator from the SH, where $1/m$ is everywhere unity. If grid compression were applied, there would still be a discontinuity of relative grid size and a variation of meridional resolution with longitude.

Figure 6 was designed in an attempt to match the appearance of an earlier version of the LODYC grid, illustrated by Marti *et al.* [12], which uses the same polar positions and resolution. In both constructions the grid parallels consist of embedded circles, but in the latter the centres are chosen in such a way that the grid spacings everywhere change continuously; this has made it possible to employ grid compression sensibly in the equatorial zone. The comparison also draws attention to the fact that the grid of Marti *et al.* is not orthogonal in the curvilinear region; this is a fault that has since been corrected. In the current grid configuration described by Madec and Imbard [11], the north pole has been moved into western China at the lower latitude of 40°N. The rationale has apparently been to keep the pole and the worst features of the grid behaviour as far from the oceans as possible and to maintain a minimum grid spacing in ocean areas equal to that used in the equatorial zone ($\frac{1}{2}$ deg. lat.); however, the change does seem to work against the principle of limiting metric variations and has resulted in very anisotropic grid cells in the Indian Ocean.

2.2. *A Reprojected Rotated Grid*

The grids of Deleersnijder *et al.* [4] and Eby and Holloway [5] are also composite grids, but they differ from the one shown in Fig. 6 in that there is a reversal in the rôles of latitude and longitude at the connection line; Eby and Holloway refer to this arrangement as the ''Equatorial transform.'' With a simple rotation, the exchange is constrained to occur at the Equator, which is the only parallel of latitude (of the conventional grid) which is a great circle and can thus also be a meridian of the rotated grid. This restriction can be lifted by reprojecting the rotated hemisphere towards the North Pole so as to occupy a region bounded by a chosen parallel of latitude, ϕ_P. For a tangent

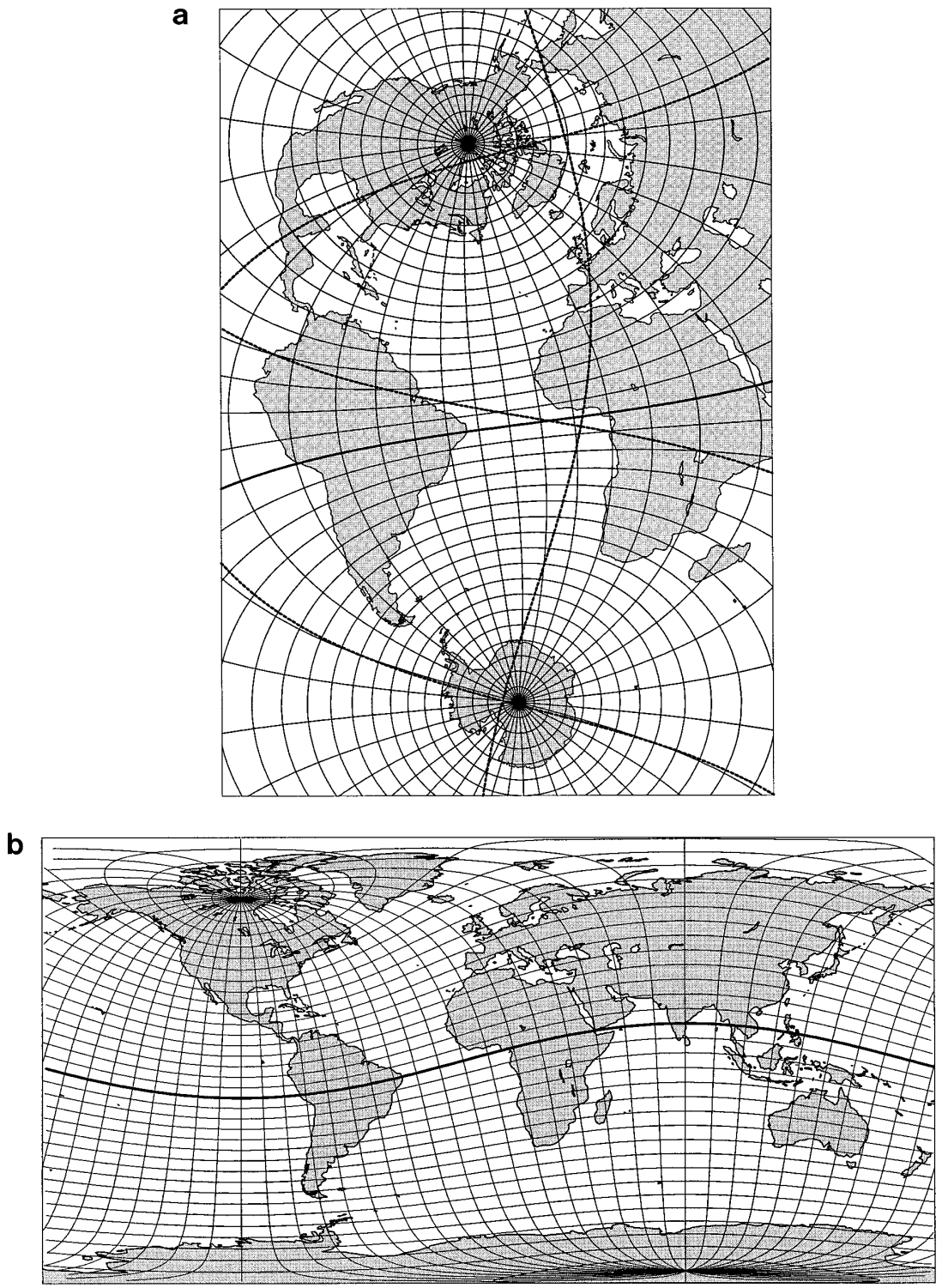

FIG. 5. The coordinate lines of a 5° × 10° bipolar grid generated about poles 160° apart at 65°N, 100°W and 85°S, 80°E: (a) oblique Mercator projection (heavy dashed lines indicate the geographical equator, prime meridian, and 90° meridians), (b) cylindrical equidistant projection. The grid equator in each diagram is indicated by a solid bold line.

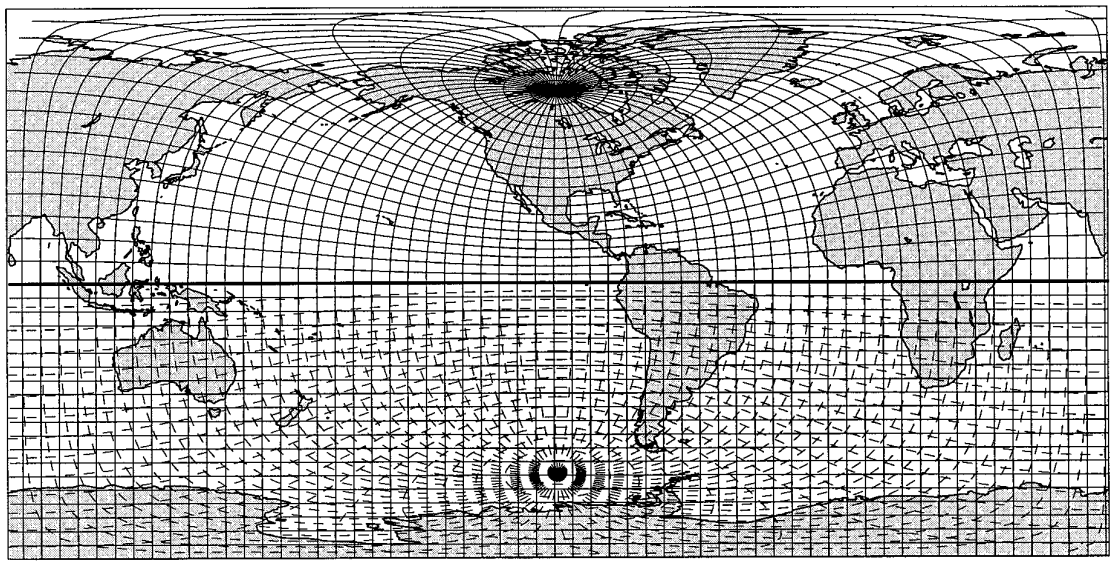

FIG. 6. The NH part of a bipolar grid with poles at 62°N and S, 101°W joined to a conventional equidistant grid in the SH. The Equator is shown as a bold line and the unused SH part of the bipolar grid as dashed lines.

point at the North Pole, the transformation described in Section 2.1 reduces to

$$\begin{aligned} \lambda_s &= \lambda_0 + 90^\circ - \text{atan2}(\sin\lambda_c, \tan\phi_c), \\ \phi_s &= 90^\circ - 2\tan^{-1}[r_P \tan(\chi_c/2)], \end{aligned} \tag{5}$$

where λ_0 is the longitude of the rotated (bipolar) equator or symmetry meridian, $r_P = \tan(\phi'_P/2)$, and

$$\chi_c = \cos^{-1}(\cos\lambda_c \cos\phi_c). \tag{6}$$

An example of a composite grid constructed by this method, with poles at 66°N, is shown in Fig. 7. The symmetry meridian has been placed at $\lambda_0 = 10°$W, which is in the centre of the North Atlantic Ocean at this latitude. The spherical meridians (λ_s) are all continuous with the parallels (ϕ_c) of the bipolar region, but the spacing of the bipolar longitudes (λ_c) at the join has been made larger than that of the spherical latitudes (ϕ_s) by a factor sec ϕ_P to give a smooth transition across the join on the symmetry meridian. In this example, $\Delta\lambda_s = \Delta\phi_c = 5°$, $\Delta\phi_s = 3°$, and $\Delta\lambda_c = 7\frac{1}{2}° \approx 3° \times \sec 66°$.

For the purpose of relating the grid to the computational array, it will be convenient to refer to the spherical meridians and their extensions as *i*-lines (i.e., grid lines constant in the index *i*) and the spherical parallels and bipolar longitudes as *j*-lines. Metric factors may be written in terms of the array coordinates ξ and η, which correspond to integral values *i* and *j* on grid lines. In the spherical region these are

$$\frac{\partial s}{\partial \xi} = a\cos\phi_s(j)\,\Delta\lambda_s(i), \quad \frac{\partial s}{\partial \eta} = a\,\Delta\phi_s(j), \tag{7}$$

and in the bipolar region,

$$\frac{\partial s}{\partial \xi} = \frac{a\,\Delta\phi_c(i)}{m(i,j)}, \quad \frac{\partial s}{\partial \eta} = \frac{a\cos\phi_c(i)\,\Delta\lambda_c(j)}{m(i,j)}, \tag{8}$$

where m is as defined by Eq. (3), with χ_c being given by Eq. (6). Equating the expressions for $\partial s/\partial\eta$ at the connection line ($\chi_c = 90°$) gives the sec ϕ_P factor referred to above. Keeping $\Delta\lambda_c$ constant in the curvilinear region (in Fig. 7) has resulted in an unequal spacing of the grid lines along the central meridian: the spacing could alternatively have been kept constant in spherical latitude, but this would have caused the grid squares near the N Pole to become somewhat elongated.

A simply rotated spherical coordinate system has the attractive feature that in the rotated region $1/m = 1$, and the metric and Coriolis factors,

$$\frac{\partial s}{\partial \xi} = a\,\Delta\phi_c(i), \quad \frac{\partial s}{\partial \eta} = a\cos\phi_c(i)\,\Delta\lambda_c(j),$$
$$f = 2\Omega\sin\phi = 2\Omega\cos\phi_c(i)\cos\lambda_c(j),$$

are, at most, products of one-dimensional variables, which would reduce storage requirements and the degree to which existing model codes would need to be modified. With reprojection, the simple form of the metric and Coriolis factors would be lost, and two-dimensional arrays

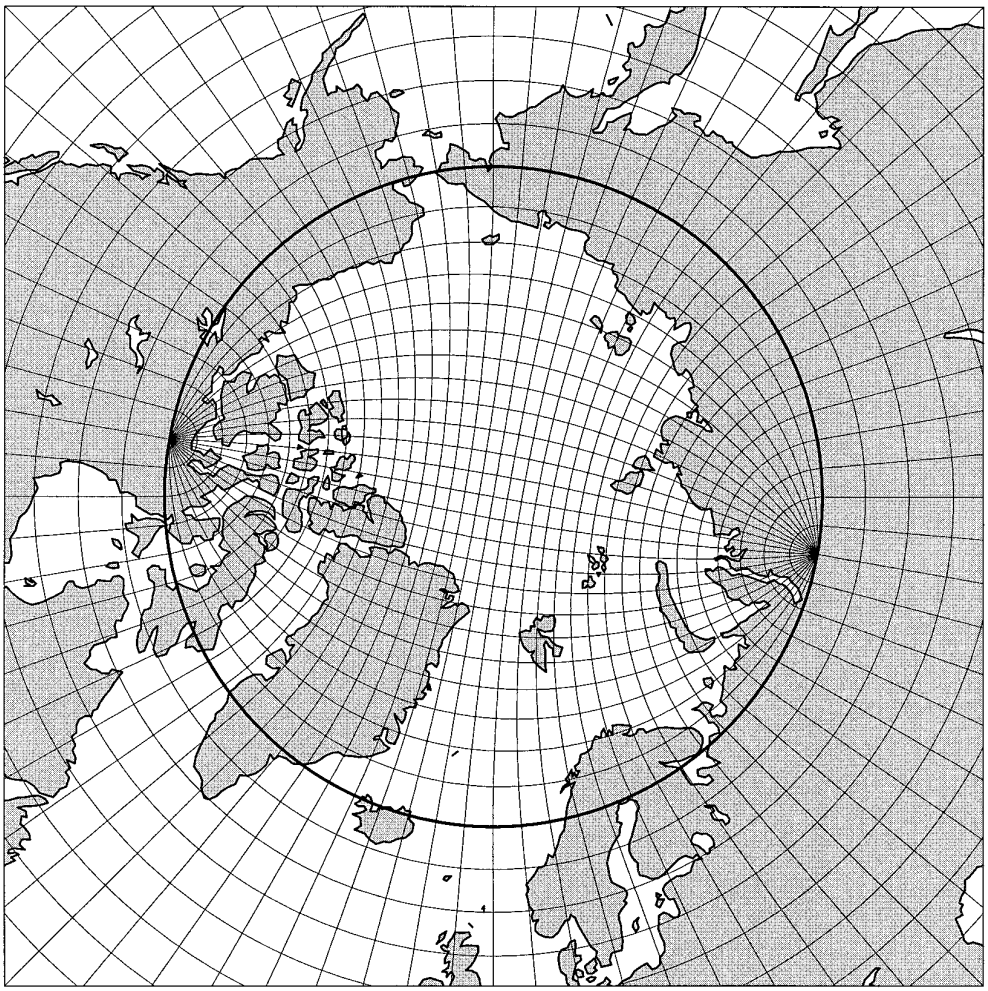

FIG. 7. A composite grid comprising a 5° × 3° latitude–longitude grid south of 66° N and the near hemisphere of a $7\frac{1}{2}$ × 5° asymmetrical bipolar grid with poles at 66°N, (10° ± 90°) W. The transition parallel is indicated by a bold circle.

would be required to store them. On the other hand, these quantities could all be precalculated, as could also any derivative expressions of the metric coefficients that might be needed. Reprojection would also create the need to recast the model equations in curvilinear form, but one would then have the compensating advantage of being able to perform the same set of calculations over the entire ocean grid, rather than essentially running two separate models on different subgrids and applying a special treatment of the scaling factors at the Equator. Deleersnijder *et al*. [4] point out that the model equations in curvilinear coordinates are not greatly different from their spherical counterparts and suggest treating the two spherical subdomains of their rotated (but not reprojected) grid as a single curvilinear coordinate system; however, this step has not been taken in the model implementations of Eby and Holloway [5] and Coward *et al.* [3].

The placing of a transition at a relatively high northern latitude would confer a number of advantages. First, it would allow nearly all of the world ocean to be modelled on a conventional grid, leaving only about $3\frac{1}{2}$% of the ocean area or about 10% of ocean points (in the case of ϕ_P = 66°) to lie in the curvilinear region; this could be a deciding factor in coupled atmosphere–ocean modelling applications because of the reduced area over which surface boundary exchanges would need to be interpolated. Second, it would allow greater resolution in the polar region than would be available with an equatorial connection, but without incurring problems of severe grid line convergence; such a configuration would be very suitable for a global ocean model with interactive sea ice. Third, in many model configurations it is the practice to make $\Delta\lambda_s$ somewhat larger than $\Delta\phi_s$, as this is considered a more efficient use of resolution when property variations are predominantly meridional; at high latitudes in the rotated region, especially away from the symmetry meridian, the grid rect-

angles would be inconveniently elongated in the E–W direction with an equatorial connection, but would be almost square if the connection were made near 60°N.

A further possible advantage of having the join at a latitude of about 60° is that, since both grid poles would lie over land (which would not be the case with a join at the Equator), the Atlantic and Pacific sectors would not need to be differently gridded, and there would be nothing to preclude the opening of the Bering Strait. While most modellers do not consider the flow through the strait to be climatically significant, Reason and Power [15] have found it to contribute an extra 8% to the modelled overturning associated with North Atlantic Deep Water formation and recommend that it be included in models used for studying climate change. Their experiments were performed on a coarse resolution (3.2° × 5.6°) spherical grid, with no special treatment of the polar region and with restoring surface boundary conditions. It would be interesting to see how their conclusions would be affected by the inclusion of an improved coordinate scheme and interactive sea ice. The opening of the Bering Strait would create the need for a reentrant boundary condition in the north–south direction, but such a condition would be useful anyway, even if the strait were closed, in order to allow the northern boundary to be placed on a cut made along the central meridian of the bipolar grid. This would keep the array rectangular and thus reduce storage requirements and allow for more efficient processing. The reentrant conditions for this configuration can be written

$$q(i,j) = q(n_i + i, j) \qquad \text{(E–W)},$$
$$q(i,j) = q(n_i - i, 2n_j - j) \times i_{\text{sym}} \qquad \text{(N–S)},$$

where q is any quantity, $i_{\text{sym}} = 1$ (-1) for a scalar (vector), 0 and n_i are the i-indices of the $(\lambda_0 - 90°)$ meridian in the spherical region, and n_j is the j-index of its geographical extension as the central meridian of the bipolar region.

The exchange of coordinate rôles creates a variation of relative grid size across the join. In the spherical region the grid spacing in the N–S direction is constant in longitude, but in the rotated region it varies with position along the connection line as cos ϕ_c $(= \cos[\lambda_s - \lambda_0])$; the same relation applies at mid-latitudes (Eq. (8)). Deleersnijder *et al.* [4] have suggested choosing an increment of grid longitude which minimises the mean square of the error $(\Delta\phi_s - \Delta\lambda_c \cos\phi_c)$ over the width of the ocean basin. Eby and Holloway [5] have remarked that for an ocean basin extending 30° on either side of the symmetry meridian, the fractional variation in grid size would be $1 - \cos 30° \approx$ 13% and have compared the equilibrium solutions of a box model using standard, rotated, and composite grids. The results of their experiments and those of Coward *et al.* [3], who studied the propagation and symmetry of equatorial Kelvin and Rosby waves using a denser (1°) version of the same grid, suggest that the effects of a join at the Equator upon model simulations would probably not be very great; there is no reason to think that the same conclusion would not apply to a transition in the mid-North Atlantic.

While the impact of metric discontinuities associated with grid rotation may be small, it would nevertheless be preferable if the suddenness of the change in grid size could be minimised as much as possible. This can in fact be done by rearranging the grid in the vicinity of the join in such a way as to expand the transition between the spherical and rotated grids from a single parallel of latitude to a zone of finite latitudinal width, across which the grid spacing can be made to change continuously. The j-lines remain circles, as before; however, the i-lines are not circular, but must be constructed in such a way as to cross the j-circles at right angles. This is essentially the same idea as has been used by Madec and Imbard [11], but the method of embedding the circles (or *semicircles*) and integrating the orthogonal trajectories is different; details of this are given in the Appendix. A rotated reprojected grid with a transition zone is shown in Fig. 8.

3. CONFOCAL GRIDS

3.1. *Grids Composed of Conic Sections*

It is possible to produce a lattice very similar to those shown in Figs. 7 and 8 from families of confocal ellipses and hyperbolae, which happen to have the property of intersecting at right angles. Such a grid would have the advantage of being global and free of discontinuities associated with patching. The reentrant conditions would be the same as given for the rotated grid.

The curves are constructed on a NH stereographic projection about foci, F_1 and F_2, lying on either side of the N Pole (N), which is the origin of the projection (Fig. 9). The foci are situated at latitude ϕ_F (or at a distance $r_F = \tan[\phi'_F/2]$ from the N Pole on the projection plane) and 90° east and west of the symmetry meridian, which is at longitude λ_0. The focal arc and the symmetry meridian define the x and y axes, respectively. Relative to these axes, an hyperbola asymptotic to the meridian at longitudes $(\lambda_0 + \lambda_c)$ and $(\lambda_0 + \pi - \lambda_c)$ has the equation

$$\frac{x^2}{r_F^2 \sin^2\lambda_c} - \frac{y^2}{r_F^2 \cos^2\lambda_c} = 1 \qquad (9)$$

and intersects the x-axis at $x = r_F \sin\lambda_c$.

It will be convenient to refer to the hyperbolae as the meridians of the curvilinear grid and to the ellipses as the parallels. The two sets of curves are not only orthogonal but have the further property of producing a conformal grid if selected such as to be equidistant in "grid longitude,"

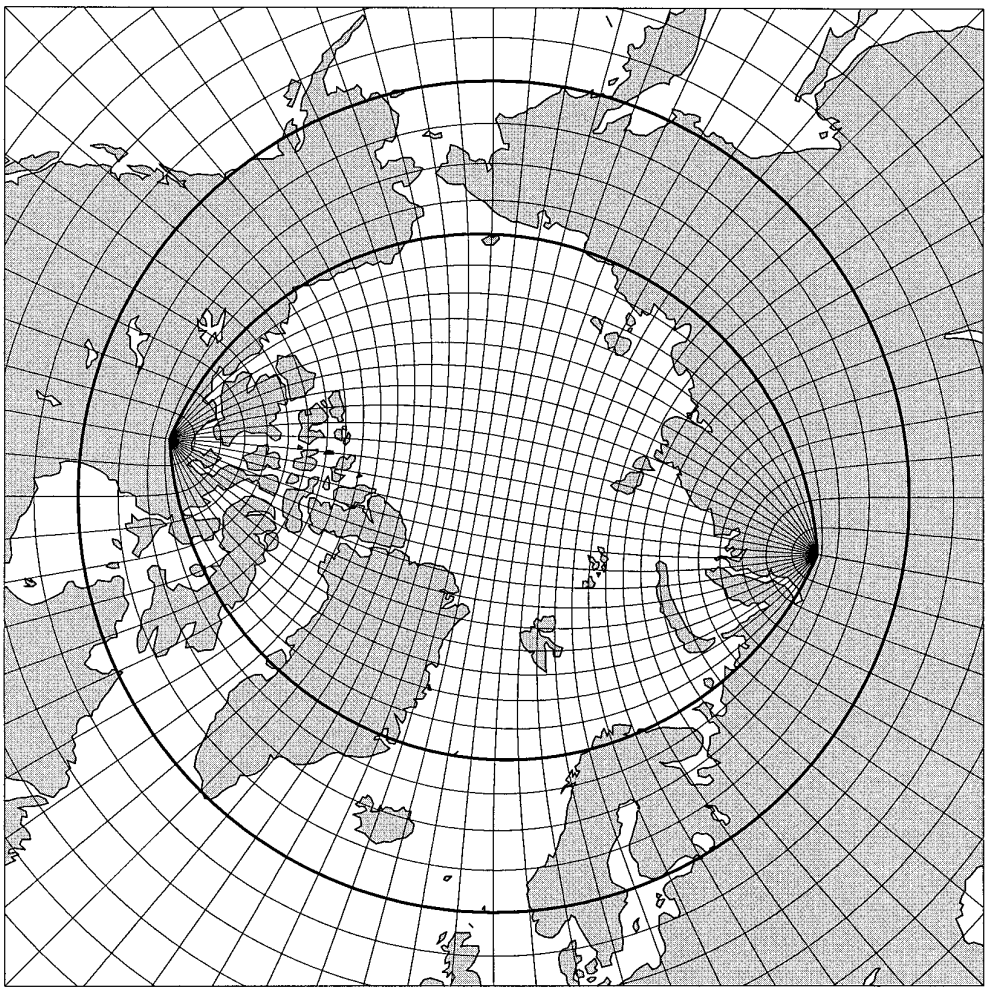

FIG. 8. A composite grid constructed as in the previous figure but with a transition region indicated by the area between the bold lines.

λ_c, and an isometric meridional coordinate, designated ψ_c. Along $x = 0$ ($\lambda_c = 0$),

$$\frac{\partial y}{\partial \psi_c} = \frac{\partial x}{\partial \lambda_c} = \frac{\partial}{\partial \lambda_c}\left(\sqrt{r_F^2 + \frac{y^2}{\cos^2 \lambda_c}} \sin \lambda_c\right) = \sqrt{r_F^2 + y^2},$$

which is satisfied by $y = r_F \sinh \psi_c$. This is the minor axis of the intersecting ellipse, the major axis being of length

$$\sqrt{r_F^2 + r_F^2 \sinh^2 \psi_c} = r_F \cosh \psi_c.$$

The equation to the family of ellipses is thus

$$\frac{x^2}{r_F^2 \cosh^2 \psi_c} + \frac{y^2}{r_F^2 \sinh^2 \psi_c} = 1. \tag{10}$$

After eliminating y and x in turn from Eqs. (9) and (10) and applying standard identities, one obtains the following expressions for the cartesian coordinates:

$$x = r_F \sqrt{\frac{(\sinh^2 \psi_c + \cos^2 \lambda_c)}{(\tanh^2 \psi_c + \cot^2 \lambda_c))}} \operatorname{sign}(\lambda_c) = r_F \sin \lambda_c \cosh \psi_c,$$
$$y = r_F \sqrt{\frac{(\cosh^2 \psi_c - \sin^2 \lambda_c)}{(\coth^2 \psi_c + \tan^2 \lambda_c))}} \operatorname{sign}(\psi_c) = r_F \cos \lambda_c \sinh \psi_c. \tag{11}$$

The derivatives of these expressions may be used to obtain the metric coefficients (which are equal, since the grid is conformal),

$$\frac{\partial s}{\partial \psi_c} = \frac{\partial s}{\partial \lambda_c} = \frac{1}{m}\left[\left(\frac{\partial x}{\partial \lambda_c}\right)^2 + \left(\frac{\partial y}{\partial \lambda_c}\right)^2\right]^{1/2}$$
$$= \frac{r_F}{m}\sqrt{\cos^2 \lambda_c + \sinh^2 \psi_c}, \tag{12}$$

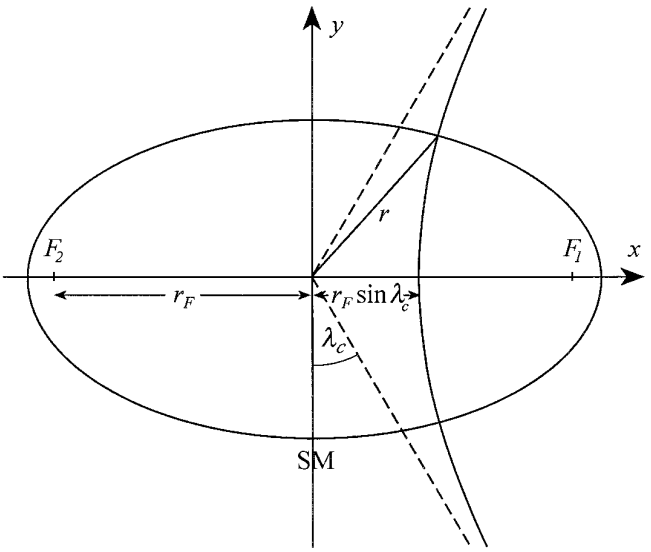

FIG. 9. Variables used for a grid composed of ellipses and hyperbolae generated around foci F_1 and F_2 at colatitude ϕ'_F. SM denotes the symmetry meridian.

where

$$m = \frac{dr}{a\,d\phi'} = \frac{d}{a\,d\phi'}\tan(\phi'/2) = \frac{\sec^2(\phi'/2)}{2a} = \frac{1+x^2+y^2}{2a} \tag{13}$$

is the map factor for a polar stereographic projection, scaled as in Section 2, and ϕ' is the colatitude. Near the foci the grid spacing,

$$\frac{\partial s}{\partial \lambda_c} \approx \frac{r_F}{m}\sqrt{\lambda_c'^2 + \psi_c^2} \approx \frac{1}{m}\sqrt{2r_F\sqrt{(x-r_F)^2+y^2}},$$

decreases as the square root of the distance from the focus, which is less sudden than the linear decrease in the case of a pole.

In addition to the two foci, there is a third singularity, at the S Pole (S), which emerges when the grid is reprojected onto the globe. To avoid having a concentration of parallels near the S Pole, it may be preferred to have a grid which is equiangular in "grid latitude" ϕ_c (i.e., latitude on the prime meridian), using the substitution,

$$r_F \sinh\psi_c = \tan(\phi'_c/2). \tag{14}$$

A grid of this type is shown in Fig. 10. Differentiation of Eq. (14) gives an expression for $d\psi_c/d\phi_c$, which can be used with $\partial s/\partial\psi_c$ from Eq. (12) for evaluating the meridional metric coefficient in terms of ϕ_c:

$$\frac{\partial s}{\partial \phi_c} = \frac{-\sec^2(\phi'_c/2)}{2\sqrt{r_F^2 + \tan^2(\phi'_c/2)}}\frac{\partial s}{\partial \psi_c}. \tag{15}$$

Because there is no discontinuity of grid size caused by patching, there is no necessity to align the y-axis with the middle of the Atlantic at any particular latitude; in Fig. 10 it has been placed 25°W in order to achieve a better alignment with coasts and curent directions in the Arctic Ocean. More generally, the whole construction could be rotated and reprojected so as to place the three singularities at any desired locations on the Earth's surface. The composite grid described in Section 2.2 could be similarly transformed, provided that appropriate care were taken in locating the symmetry meridian.

It will be noticed that the spacing of the meridians along the focal axis decreases from a maximum at the N Pole to zero at the generating foci; this contrasts with a slight increase of spacing in the rotated grid case (Fig. 7). For a given latitude of the northern singularities and given global resolution, the confocal grid is somewhat coarser than the rotated grid over most of the Arctic Ocean. Whether or not this property would be advantageous would depend upon whether numerical stability or resolution in the sea ice region were the more critical requirement.

At large distances from the N Pole, the coordinates become asymptotically aligned with those of a spherical grid. With $\phi_F = 60°$, the variation of latitude of the parallels near the Equator is only ±1°, which probably would not preclude the use of grid compression there.

3.2. *Doubly Periodic Lattices*

If it were necessary, one could modify the grid in such a way as to enforce an east–west orientation at the Equator or along some chosen latitude circle, while at the same time keeping the grid everywhere orthogonal; this would allow the grid to be used as part of a composite scheme in a manner similar to that envisaged in Section 2.2. One way of doing this would be to generate a conformal grid about *two* pairs of foci, symmetrically placed in northern and southern hemispheres. The meridional great circle comprising the focal arcs would divide the sphere into two hemispheres, and the four foci themselves would mark the corners of two rectangular arrays, joined back to back. The problem is how to map each rectangle conformally onto a circle representing one hemisphere of a polar stereographic projection. For the case of foci 90° apart, the transformation is the inverse of Goyou's projection of a hemi-

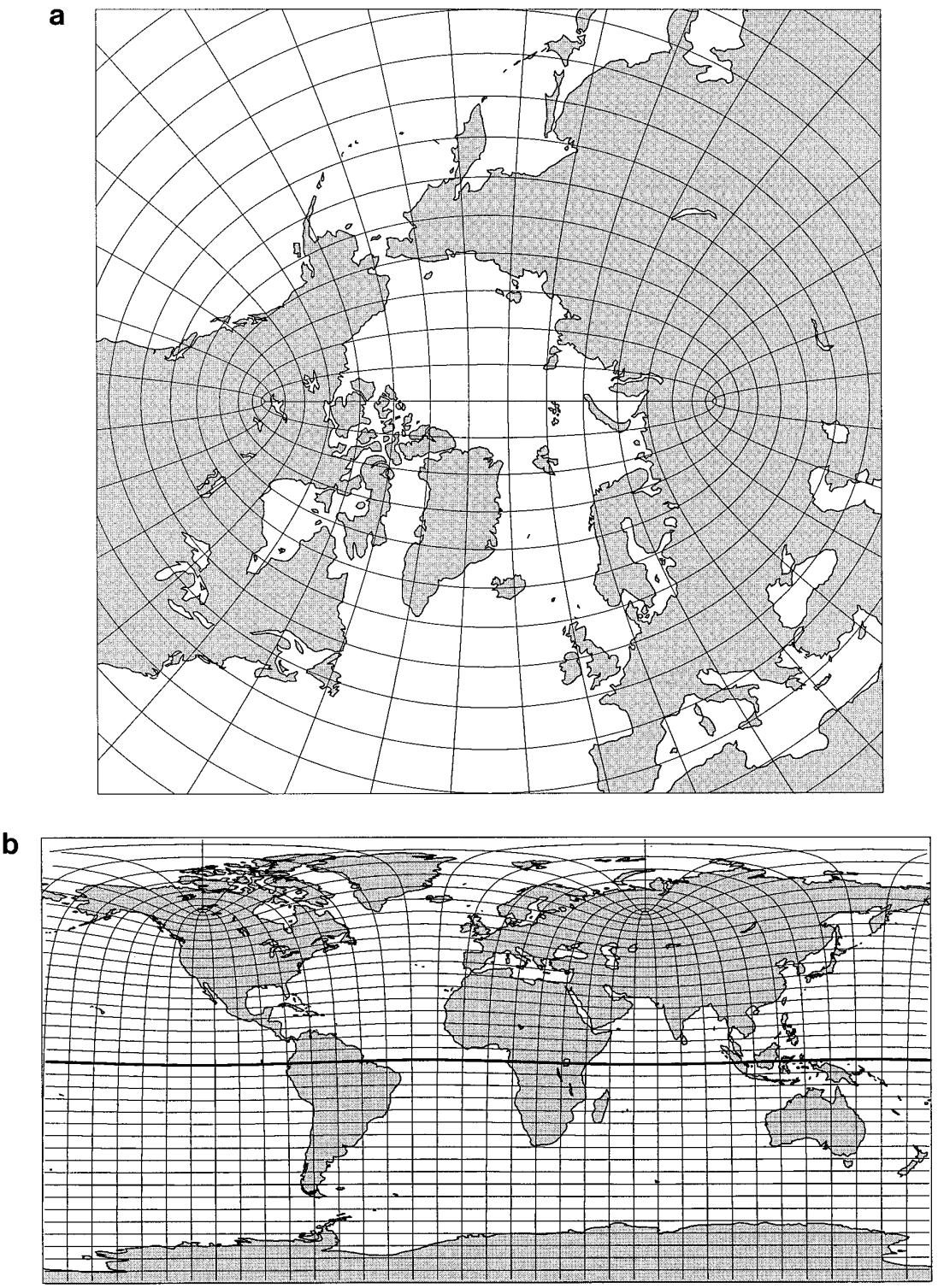

FIG. 10. (a) A grid composed of ellipses and hyperbolae having foci at 60°N, (25° ± 90°) W, superimposed on a NH polar stereographic projection (aligned with the symmetry meridian). The ellipses are spaced 5° apart on the central meridian and the hyperbolae are asymptotic to a 10° spacing of meridians at distance. (b) The lattice as it appears on a cylindrical projection, with a bold line showing the "grid equator," which touches the geographical equator at 25°W and 155°E.

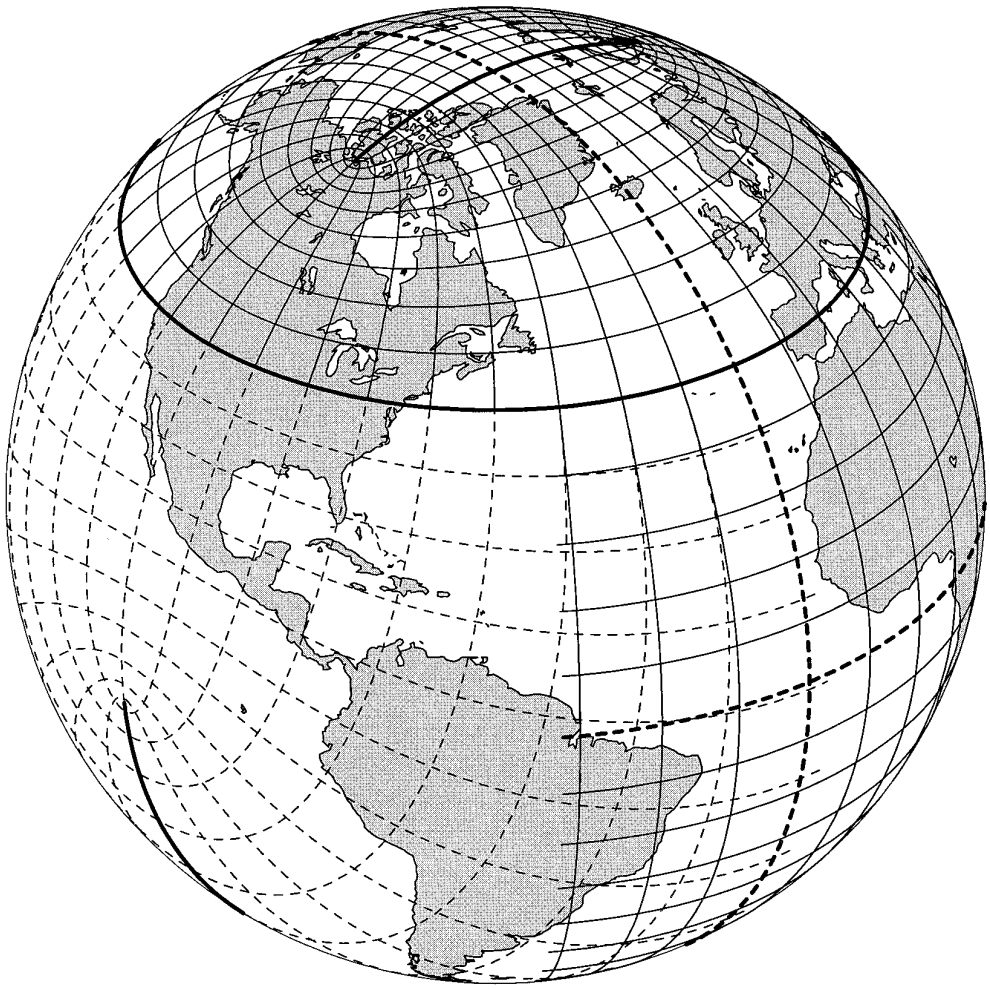

FIG. 11. A grid generated about two focal arcs (bold lines), one spanning the North Pole and the other (partly obscured) the South Pole. The reprojected ''equator'' of the grid (bold circle) lies along the 40°N parallel. South of this line are shown parts of two graticules: the unused southern part of the curvilinear grid (dashed) and an $8° \times 10°$ spherical grid which is designed to replace it. The Earth's equator and the symmetry meridian (20°W) are indicated by bold dashes. (Oblique orthographic projection.)

sphere within a square, and the grid coordinates may be evaluated from a complex series derived from Schwarz's integral (Lee [10, pp. 68–71]).

For use in a composite grid, the construction would need to be reprojected northward and the zonal grid spacing adjusted to allow it to be connected to a regular latitude–longitude grid. In the example shown in Fig. 11, the grid equator has been placed on 40°N. There is a small grid size discontinuity at the join, which could be smoothed, if required, using techniques similar to those described in the Appendix or by Madec and Imbard [11]. To minimise the areal extent of the curvilinear region, the connection line could conceivably be located nearer to the northern foci than has been shown here; this would require a mapping which would allow the square arrangement of the foci in the unreprojected transformation to be generalised to a rectangular one. It would not serve any purpose to elongate the rectangle too much, however, as this would tend to result in grid lines similar in appearance to those shown in Fig. 8 and a loss of the desirable resolution properties near the Pole. For constructing a composite grid with a small curvilinear region or a highly resolved Arctic region, the reprojected rotated grid probably represents the most economical arrangement; a conic section grid or other confocal coordinate scheme is probably best used where a single global grid is required for ocean or ice–ocean modelling without atmospheric coupling.

In addition to Goyou's projection, there are a number of other ''doubly periodic'' projections that have been devised, mostly by Lee [10], based on Jacobian and Dixon elliptic functions, for conformally mapping the sphere onto polygons and polyhedra; some of these, in inverse form, could be considered for global grids. The grids in question are characterised by special points of the focal type—

actually, the curves are not conic sections, and the word "focus" is used somewhat loosely here to refer to a particular type of singularity in which the grid lines forming a corner of the array flatten into a straight line in physical space. This sort of device is sometimes employed in boundary fitting schemes to create a grid corner on a smooth boundary; examples of the ways in which it can be used are illustrated by Thompson *et al.* [20]. In the present study the aim has been to keep all singular points well away from the ocean domain. With an increase in their number this might be difficult (a cubic mapping would have eight); however, the admission of foci as interior points would not necessarily be as troublesome as one might expect. Because a focus is not a finite source of coordinate lines, the lines of the grid do not converge so abruptly upon this type of singularity as upon a pole, and their spacing remains tolerable at a closer approach to it. Rančić *et al.* [14] have recently modelled the shallow water equations using a grid conformally mapped onto an expanded spherical cube.

4. MULTIPOLAR GRIDS

A conformal latitude–longitude grid can be constructed by choosing the parallels of latitude to have an equal spacing of the "isometric latitude," $\psi(\phi)$, defined such that

$$\Delta\psi = \Delta\lambda = \Delta\phi/\cos\phi$$

(Lee [10]), where (λ, ϕ) are the coordinates of a point X. Integration w.r.t. ϕ gives the Mercator projection equation,

$$\psi = \log\tan(\phi/2 + \pi/4); \tag{16}$$

and a grid equidistant in λ and ψ may be referred to as a Mercator grid. Equation (16) can also be rendered

$$\psi = \log\tan(\rho_S/2) = -\log\tan(\rho_N/2), \tag{17}$$

where ρ_S and ρ_N are the angular distances $(\pi/2 \pm \phi)$ of X from the N and S Poles, respectively. The function ψ has the property that its Laplacian,

$$\nabla^2\psi = \frac{1}{a^2\cos\phi}\frac{d}{d\phi}\left(\cos\phi\frac{d\psi}{d\phi}\right)$$

is zero everywhere except at the Poles, where its integral over the solid angle circumscribed by a parallel at latitude ϕ may be evaluated using the divergence theorem and the fact that $d\phi = d\rho_S = -d\rho_N$. Around the S Pole,

$$\int_0^{\rho_S}\int_0^{2\pi}\nabla^2\psi\,(a\sin\rho\,d\lambda)\,a\,d\rho = \int_0^{2\pi}\left(\frac{1}{a}\frac{d\psi}{d\rho}\right)_{\rho=\rho_S} a\sin\rho_S\,d\lambda$$
$$= \frac{1}{\sin\rho_S}\times 2\pi\sin\rho_S$$
$$= 2\pi.$$

The integral around the N Pole is -2π. These relations indicate that parallels of latitude, when chosen to give a conformal spacing, can be considered to fulfil a rôle similar to that of equipotentials lying between infinite parallel wires in electrostatics.

The form of Eq. (17) suggests the decomposition

$$\log\tan(\rho_S/2) = \log\sin(\rho_S/2) - \log\cos(\rho_S/2)$$
$$= \log\sin(\rho_S/2) - \log\sin(\rho_N/2),$$

which further suggests that each component may be treated to some extent independently as defining a sort of "monopole" field,

$$\psi_k = -q_k\log\sin(\rho_k/2), \tag{18}$$

where ρ_k is the angular distance of X from pole k. I say "to some extent," because the permissibility of doing this will depend upon the divergent properties of $\nabla\psi_k$. The latitudinal gradient of ψ_k (away from the poles themselves) is

$$\frac{1}{a}\frac{d\psi_k}{d\rho_k} = -\frac{q_k}{a}\frac{d}{d\rho}\left(\sin\frac{\rho_k}{2}\right) = \frac{-q_k}{2a\tan(\rho_k/2)}, \tag{19}$$

and the Laplacian is

$$\nabla^2\psi_k = -\frac{q_k}{a^2}\frac{1}{\sin\rho_k}\frac{d}{d\rho_k}\left(\sin\rho_k\frac{d}{d\rho_k}\left(\log\sin\frac{\rho_k}{2}\right)\right) = q_k/2a^2,$$

except at the poles, where the integral of the Laplacian is

$$\int_0^{\delta\rho_k}\int_0^{2\pi}\nabla^2\psi_k(a\sin\rho\,d\lambda)\,a d\rho = \int_0^{2\pi}\frac{1}{a}\frac{d\psi_k}{d\rho_k}(a\sin\delta\rho_k\,d\lambda)$$
$$\to -2\pi q_k \quad (\delta\rho_k\to 0),$$

which is incidently the negative of the integral over the rest of the sphere. Although the N and S monopole fields do not *individually* satisfy Laplace's equation, it can easily be seen that they do so in combination, provided that their pole strengths be made equal and opposite. The Mercator projection equation (Eq. (16)) results from assigning $q_N = 1$ and $q_S = -1$, and by placing the poles in their usual geographical positions.

There is no particular reason why the poles should be placed 180° apart; the only requirement is that they be equal and opposite. The polar distances used in the Eq. (18) would then be ρ_1 and ρ_2, as shown in Fig. 4b; these angles are measured along great circle arcs on the true sphere (not along the grid meridians) and are given by

$$\rho_k = f_c(\lambda_k - \lambda, \phi'_k, \phi'). \tag{20}$$

The potential distribution of two asymmetrically disposed monopoles can be shown to be the same as that of a bipolar grid with the same polar positions.

One could, in principle, use the potential field to construct the entire curvilinear grid; however, the determination of longitudes would require numerical integration of partial differential equations. There would be little point in doing this for setting up a bipolar grid, which can be generated directly by the method of reprojection given in Section 2. But with the potential formulation one is not limited to a choice of two poles; one could construct a potential field from any arbitrary distribution of poles, the only restriction being that the sum of the pole strengths be zero (which means that there must be at least two poles). This condition is necessary since the Laplacian of the total field at nonpolar locations,

$$\nabla^2\psi = \Sigma\nabla^2\psi_k = \Sigma q_k \nabla^2 \log \sin(\rho_k/2),$$

must be zero for conformality. A multipolar distribution could, of course, be equivalently made up from a summation of balanced bipolar fields, but, for the purpose of specification and computation, the monopole formulation is more convenient.

Parallels and meridians are constructed by integrating the local coordinates, $d\mathbf{x} = d(x, y) = (a\cos\phi_s\, d\lambda_s, a d\phi_s)$, using their derivatives w.r.t. λ_c and ψ, viz.,

$$\int \frac{\partial \mathbf{x}}{\partial \lambda_c} d\lambda_c = \int \frac{(\cos\gamma, -\sin\gamma)}{|\nabla\psi|} d\lambda_c,$$

$$\int \frac{\partial \mathbf{x}}{\partial \psi} d\psi = \int \frac{(\sin\gamma, \cos\gamma)}{|\nabla\psi|} d\psi$$

(see Fig. 12). Here, γ is the bearing of field vector, $\nabla\psi$, which is defined by

$$\nabla\psi = (\sin\gamma, \cos\gamma)|\nabla\psi| = \sum_k (\sin\gamma_k, \cos\gamma_k)\frac{1}{a}\frac{d\psi_k}{d\rho_k},$$

where $d\psi_k/d\rho_k$ is given by (19) and ρ_k by (20), and

$$\gamma_k = f_t(\lambda_k - \lambda, \phi'_k, \phi') \tag{21}$$

is the bearing of pole P_k. The metric coefficients are just

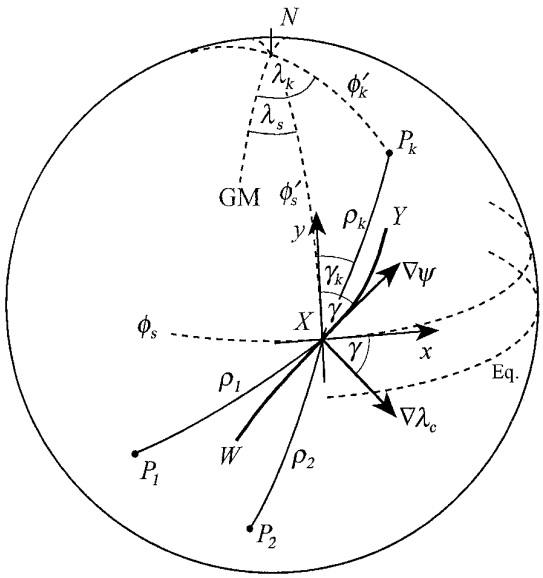

FIG. 12. Angles, grid vectors, and tangent plane coordinates at a point $X(\lambda_s, \phi_s)$ associated with a grid generated by poles P_1, P_2, ..., P_k, ... The curve WXY is a grid meridian: in the bipolar case it would be the small circle arc P_1XP_2.

$$\frac{\partial s}{\partial \lambda_c} = \frac{\partial s}{\partial \psi} = \frac{1}{|\nabla\psi|}. \tag{22}$$

If the meridional coordinate be expressed as an equivalent latitude, the meridional derivatives and metric are

$$\frac{\partial \mathbf{x}}{\partial \phi_c} = \frac{1}{\cos\phi_c}\frac{\partial \mathbf{x}}{\partial \psi}, \quad \frac{\partial s}{\partial \phi_c} = \frac{1}{\cos\phi_c}\frac{\partial s}{\partial \psi}. \tag{23}$$

In practice, the grid lines in the i and j directions were extended using a fourth-order Runge–Kutta scheme. To prevent inaccuracies due to the convergence of meridians, the integration of x and y from each grid point was referred to the local (departure point) polar stereographic projection plane, with an appropriate scaling of $\nabla\psi$.

The expressions given in the preceeding paragraphs for grid poles on a spherical surface are analogous to those applicable on a Cartesian plane, except that γ_k is calculated by spherical geometry (Eq. (21)) rather than plane geometry (atan2(x, y)), and the expression (log sin(ρ/2)) for the potential takes the place of (log r) for the potential around a pole in two-dimensions. The integration of the coordinate lines could, in principle, be carried out on a polar stereographic projection, using the equivalent Cartesian expressions (in this case, there would be no need to prescribe a balance of pole strength, since any imbalance would create a compensating pole at infinity rather than a dispersed distribution). However, the integration might not be very

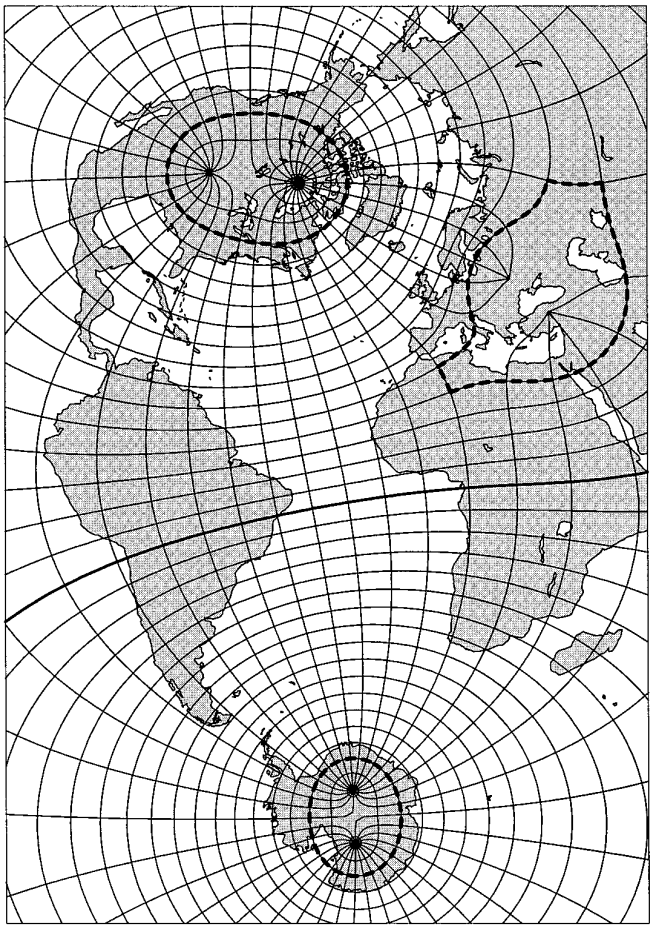

FIG. 13. A notional $5° \times 10°$ multipolar grid generated by a pair of north poles over North America ($q_k = 0.6, 0.4$), a pair of south poles over Antarctica ($q_k = -0.5, -0.5$), and a dipole over eastern Europe ($q_k = \pm 0.3$). The grid lines enclosed within heavy dashed curves connect points computed by the scheme but excluded from the rectangular computational array. (The projection is as for Fig. 5a.)

accurate or efficient at large distances from the projection pole.

An example of the type of grid that can be generated from a number of poles is shown in Fig. 13. The basic layout is similar to that shown in Fig. 5a, but the poles over Antarctica and North America have been divided to improve the alignment of the grid lines with their coasts. A dipole over eastern Europe has been added to bunch the parallels over the Norwegian Sea somewhat and to reduce the number of unused grid points over Asia. While advantageous modifications to the grid alignment can thus be made locally, it is not possible to apply them independently across the globe. In practice, also, it is important to avoid having singularities and nodal points within or close to the computational domain. For global grids, this essentially means restricting separate aggregations of (net) pole strength to a couple of well-defined continental ''polar'' regions. The computational grid can then be represented by a rectangular array with just the normal periodic boundary conditions in the east–west direction. In the above example, the dashed boundaries over North America and Antarctica represent the ''northern'' and ''southern'' boundaries of the grid array; a dashed boundary over Eurasia also excludes an area where a dipole would cause ambiguous indexing of grid points. The polar aggregations have been normalised to ± 1, and a one-dimensional stretching of ψ has been applied using Eq. (16) to give a regular 5° notional latitude increment.

Because of the limitations referred to, the grids that can be usefully generated by the superposition of a *finite number* of monopole fields do not greatly extend the advantages of the bipolar grid. On the other hand, the multipolar formulation is one that can be applied conceptually to cases of a continuous distribution of pole strength. As in the Cartesian analogue, the field of an arbitrary distribution of pole strength confined by an equipotential can equivalently be represented by that of a linear distribution of pole strength along the equipotential. This applies as much to longitude as to latitude lines. When the equipotential is determined from a known distribution, the linear density can be diagnosed as $|\nabla\lambda_c|/(2\pi)$, where $|\nabla\lambda_c| = |\nabla\psi_c|$ is the conformal grid line concentration. When the bounding equipotentials are arbitrarily placed, as is usually the case in hydrodynamical problems, this cannot be done, and the interior grid point positions must be solved as a boundary value problem.

In certain instances, the bounding equipotential may collapse to a single line of pole strength. On a Mercator grid, for instance, the meridians may be considered to be equipotentials generated by linear distributions of density $\partial\lambda/\partial x = \pm 2 \sec \phi$, along (any) two meridional arcs. On the confocal grid defined by Eq. (11), the ellipses (ψ_c) are equipotentials generated by a linear distribution of pole strength along F_1F_2 and an equal and opposite point pole at S; the hyperbolae (λ_c) are generated by equal and opposite distributions along F_1S and F_2S. This interpretation may readily be extended to doubly periodic meshes. On each of these grids, the polar arcs are linear singularities at which the potential gradient abruptly changes sign but not magnitude; however, the arcs need not be excluded from the ocean domain on that account since, for practical purposes, the grid can be regarded as continuously conformal if an appropriate sign convention (reentrant boundary condition) be adopted. In principle, linear singularities could be incorporated into numerically generated grids, given suitable methods for matching grid lines across them in the spherical domain.

5. CONCLUSION

Three approaches to numerical grid generation have been used, based on the explicit use of properties of confor-

mal map projections. All result in grids which have a smooth variation of grid size and orientation and which remove singularities from the ocean areas. Because of their analytical basis, problems of matching grid lines at reentrant cuts are not encountered.

The several individual coordinate schemes that have been proposed embody two basic configurations. The first involves a shift of one or both poles into a nondiagonal arrangement and is represented by the asymmetrical bipolar grid. The basic design can be varied by the specification of polar distributions in place of a single pair of opposite poles, using the formulation of Section 4, but the poles need to be essentially restricted two polar land regions in order to keep the grid well-behaved over the oceans. Dipoles may be used to focus grid lines in particular ocean areas. The second configuration is one in which the function of one pole is taken over by a pair of foci lying on either side of its former position. This design has three singularities and is typified by a grid composed of confocal ellipses and hyperbolae. Although differently constructed, a 90°-rotated (and reprojected) hemisphere of a latitude–longitude grid joined to an unrotated spherical grid would have the same practical properties. Both configurations can be represented on rectangular arrays and only require the application of fairly straightforward continuity conditions.

The introduction of global curvilinear grids was seen as a way of removing the polar singularity from the ocean domain and, hence, of allowing a better simulation of the Arctic circulation in global models. Another, perhaps fortuitous, outcome of this is that, in some of the examples considered (Figs. 7, 8, and 10), the coordinate lines, while not converging to a point or so closely as to create a need for Fourier filtering, do nevertheless come rather closer together in the Arctic than in other parts of the globe, and in such a way as to preserve a roughly equal spacing in the two coordinate directions. For studies in which the solution in the sea ice regions is the main point of interest, these characteristics allow one to have good resolution in the polar region, while at the same time keeping it in contact with the global ocean. Because the circulation in the Arctic is relatively sluggish, the extra resolution in this region will not necessarily be a limiting factor on the model time step.

It has been shown that the parallels of the bipolar grid, although in practice geometrically constructed, can be considered as equipotentials resulting from the superposition of two off-axis monopole fields. This is a special case; more generally, a field of equivalent isometric latitude may be generated by any arbitrary distribution of (balanced) pole strength. The explicit poles only produce the parallels; the meridians are assumed to be generated by a different and undetermined distribution of pole strength. Since this is unknown and in any case dispersed, the actual locations of grid points are found by integration of the coordinate derivatives in directions parallel and perpendicular to the field strength vector. The confocal type of grid is also one that can be understood as being generated by a particular distribution of pole strength; in this case, however, the distribution is not aggregated at the foci but is spread along the arc (or arcs) connecting them. This being the case, the latitude contours cannot be conveniently computed from a superposition of monopole fields, since there would in theory be an infinite number of them.

The advantages of the multipolar technique are somewhat limited by constraints on the distributions of discrete poles that can be chosen to give well-behaved grids. However, the formulation does have conceptual value in allowing for the generation of grids by dispersed sources, and it is reasonable to hypothesise, by appeal to the electrostatic theory, that any field generated as a solution of Laplace's equation on a portion of the sphere could, in principle, be constructed from the superposition of fields produced by appropriate distributions of balanced positive and negative pole strength on its boundaries. The multipole formulation thus provides a link between geometrical and boundary value methods of generating conformal grids on the sphere and may be a simple but useful tool for probing the wider range of configurations that one might expect to be able to generate using numerical methods.

Explicit and conformal boundary fitting methods differ chiefly in the way that they pose the grid generation problem. The former specify the positions of two, or at most a small number of, special points and maintain some control over grid line concentration by virtue of the distance from them; they only indirectly control the *alignment* of grid lines, which therefore only match coastal boundaries approximately or fortuitously: the latter fit grid lines to boundaries specifically, but they only indirectly control grid spacing. For global models, where a control of grid line concentration may be of greater importance than the conformation of grid lines to boundaries, the explicit approach may have some advantages.

A unifying factor in the explicit methods chosen for this study has been the use of the conformal properties of stereographic and Mercator map projections, which enable the specification of grids which are known *a priori* to be orthogonal. Conformal transformations preserve orthogonality in any number of successive applications. It would thus be in order to apply reprojection to any analytically or numerically generated orthogonal grid. The grids shown in Figs. 7, 8, 10, and 11 could be reprojected to allow an arbitrary placement of the three singularities; for instance, the focal arc could be repositioned to lie across Iceland and improve the resolution in the far North Atlantic. Conformal projection allows meshes constructed in Cartesian coordinates to be applied to the sphere, a facility that has been used with the confocal grids of Section 3. This may

be of some relevance for numerical grid generation. The most likely requirement is for a global ocean bounded by two passive (i.e., land) regions containing line sources. Stereographic projection could be used in such a way as to spread one such region across the far pole, thus creating an externally bounded, but doubly connected, ocean domain in plane coordinates; techniques for contouring such regions are discussed and illustrated by Ives and Zacharias [9]. In practice, some difficulties arising from the wide range of map scales generated by projection might need to be overcome.

Conformal grids (as distinct from conformal transformations) are employed in many numerical grid generation techniques because they can be obtained as solutions of elliptic boundary value problems. This consideration does not apply here; however, the construction of the multipolar grid does exploit the additive property of conformal fields, which does not apply to orthogonal fields in general. Conformality, however, is not an end in itself but simply a convenient means of ensuring orthogonality and a smooth layout of grid points. In its pure form, a conformal grid is composed of curvilinear squares. Because a strictly isometric point distribution is not always optimal for modelling, it is common in boundary fitting schemes to apply a one-dimensional differential stretching (or contraction) to one or both of the coordinates. This may be done to resolve a lateral boundary layer or to maintain a more even resolution along an irregular boundary. Obviously this must be carried out in such a way as to preserve a smooth variation in the grid spacing.

It so happens that the various global grids discussed in this article (spherical, bipolar, confocal, and multipolar) are also either conformal or stretched conformal grids; it is this property that makes all of them amenable to a field interpretation. But this is merely an interesting observation. In global modelling, the problem with isometric grids is that the *j*-lines lines become very closely spaced and numerous as the poles are approached, and it is generally better to have a more even distribution of points in each direction. For a latitude–longitude grid, an equidistant spacing is the one usually preferred, and this may be regarded as the best "stretching" of the corresponding conformal (Mercator) grid. For the curvilinear grids proposed here, a spacing equidistant in the coordinates λ_c and ϕ_c, as variously defined, might be considered appropriate. But this is a largely arbitrary matter, and there are occasions when one might wish deliberately to depart from homogeneity.

The most obvious case of this is in the practice of including a tapered increase in the density of the parallels in the equatorial zone. There are other places, such as the western boundary currents, the polar regions, and certain straits, where a *localised* enhancement of resolution might be desired, but less easily achieved. In some studies, separate grid compressions have been applied in the zonal and meridional directions. Oberhuber [13], for instance, has used them to focus grid lines in the Greenland–Iceland–Norwegian Seas. But paired compressions produce radiating bands of elongated cells and wasted resolution. This is a problem for which the use of curvilinear grids may provide an answer. With their greater range of design and greater flexibility of singular point placement, curvilinear grids widen the opportunities for a satisfactory control of resolution. Control is exercised, albeit still only broadly, in two ways: in the first instance, by the fairly natural way that the singularities affect the overall framework of grid alignment and convergence; and in the second, by the designer's use of grid compression in each coordinate direction within this framework. When the framework is right, the compression will work efficiently (or may not be needed at all). Thus, for a good resolution of the Antarctic continental shelf or the Arctic entrance seas, one might use a configuration such as shown in Fig. 5a or 13 and a compression of latitudes in the relevant polar region.

To proceed further in attempting to control resolution or accommodate competing requirements, such as a desire to impose an east–west alignment on the grid parallels over certain parts of the globe, it may be necessary to sacrifice some of the advantages of a homogeneous global grid and resort to the use of composite grids. The rotated and reprojected grid shown in Fig. 8 has been proposed as one that would (1) allow conventional coordinates to be used over most of the ocean, (2) give good resolution of the Arctic sea ice region, while overcoming the usual problems caused by the convergence of meridians near the Pole, and (3) allow Bering Strait to be opened, if desired. Composition inevitably results in some loss of continuity of metric coefficients across the joins, but this is emphatically better than the interpolative exchanges required with the overlapping grids propounded by Starius [17] and tested in an atmospheric model by Browning *et al.* [2]. In order to reduce overall truncation errors and, also, possibly to allow analytical functions to be used for grid definition and evaluation of derivatives, a spreading of the transition over a number of latitudes could be considered. In the parlance of conformal grid generation, this would amount to a spreading of coordinate line sources. An example of a configuration in which a transition zone is included has been given for the rotated grid case. Similar modifications could probably be devised for the mesh shown in Fig. 11 and other types of compound grids. The NH of the LODYC grid could be regarded as equivalent to a single large transition zone for the composite shown in Fig. 6.

Two suggestions have thus been made for extending the advantages of using a rotated grid for the North Atlantic and Arctic Oceans—one being to reproject the rotated hemisphere towards the North Pole; the other, to insert a zone of transition between the two grids so as to effect a

smooth variation in grid spacing across the join. Either solution could be implemented separately, but it would be just as easy to implement the two together, since both modifications commit the user to recasting the model equations in curvilinear coordinates. In fact, given a model of an appropriately general formulation, any curvilinear grid that can be mapped onto a rectangular array could be used. The form of the model equations is not dependent on the particular geometry of the grid; all that the model requires is a rule for applying reentrant boundary conditions and a set of metric coefficients and Coriolis factors, which need only be computed once for any configuration. Finite difference forms of the governing equations in orthogonal curvilinear coordinates are formally similar to those used with spherical models, except for the two-dimensional dependence of the scaling and Coriolis factors and the transverse–isotropic orthogonal curvilinear form of the differential operators. They have been given for the SPEM model of Haidvogel *et al.* [6] and Hedström [7], and are available for the Cox–Bryan model from the author.

When a grid is defined analytically, the metrics can likewise be obtained, by derivation of the grid equations. Analytical expressions for some of the grids have been given in Eqs. (4), (7), (8), (22), and (23). Thompson *et al.* [20] (cited by Deleersnijder *et al.* [4]) have shown that truncation errors are smaller when metric coefficients are evaluated from the finite difference expressions used in the model equations rather than from differential expressions. Since, in either case, these errors are only likely to become large close to point singularities, which are designed to be at least several grid points removed from the computational domain anyway, this would probably not be an important consideration.

Finally, it is worth summarising how well the various grids satisfy the desiderata given in the Introduction; this has been done in Table I for the various global coordinate schemes that have already been put to use and for a number of those that have been proposed here.

Note. Programs for generating the grids described in this article may be obtained by electronic mail from the author at `rjmury@mullara.met.unimelb.edu.au`.

APPENDIX

The transition zone shown in Fig. 8 is bounded on the equatorward side by a parallel of the spherical grid and on the poleward side by a meridian of the bipolar grid. Since the basically W–E coordinate lines, or *j*-lines, of the spherical grid (parallels) and the bipolar grid (meridians) are all circles, it will be sensible to make them circles in the transition region also. The extensions of the spherical meridians, or *i*-lines, cannot be so chosen but must be drawn in such a way as to cross the *i*-lines perpendicularly; they will not be circular but will have varying curvature. For constructing this type of grid one requires a procedure for

1. marking off grid intersections along the prime meridian to ensure a smooth variation in grid size between the spherical and bipolar regions;
2. placing the centres of the grid circles so as to give a smooth variation in the spacing of their arcs at all other longitudes; and
3. constructing orthogonal trajectories for extending meridians of the spherical region northward.

These operations are to be carried out on a polar stereographic projection with an x-axis on the symmetry meridian and y-axis joining the poles of the bipolar grid. The coordinates (x, y) of a point, X, on the projection plane (see Fig. A1) are given by

$$(x, y) = \tan[(90^\circ - \phi)/2](\cos\lambda, \sin\lambda). \tag{A1}$$

Step 1 is carried out by representing the latitudes, ε, of the parallels on the prime meridian in the transition zone by a cubic function whose coefficients are determined by matching it to the latitudes and their rates of change with j in the adjoining regions at the boundary lines, $j = j_1, j_2$. For calculating derivatives, it is necessary that ε be a function of a continuous variable, η, which is made to be equal to the integral values j on j-lines; ξ is similarly defined to be equal to i on i-lines. In the following equations, primes are used to denote differentiation w.r.t. η. The quantities to be matched are $\varepsilon_1 = \varepsilon(j_1)$, $\varepsilon_2 = \varepsilon(j_2)$, $\varepsilon_1' = d\varepsilon/d\eta(j_1)$ and $\varepsilon_2' = d\varepsilon/d\eta(j_2)$. The cubic may be expressed as

$$\begin{aligned}\varepsilon(\eta) = (1-\delta)\varepsilon_1 + \delta\varepsilon_2 + [(-\delta^3 + 3\delta^2 - 2\delta)\varepsilon_1'' \\ + (\delta^3 - \delta)\varepsilon_2'']\Delta j)^2/6,\end{aligned} \tag{A2}$$

where $\delta = (\eta - j_1)/\Delta j$ is an interpolant, with $\Delta j = (j_2 - j_1)$, and

$$\varepsilon_1'' = (-4\varepsilon_1' - 2\varepsilon_2')/\Delta j + 6(\varepsilon_2 - \varepsilon_1)/(\Delta j)^2,$$

$$\varepsilon_2'' = (2\varepsilon_1' + 4\varepsilon_2')/\Delta j - 6(\varepsilon_2 - \varepsilon_1)/(\Delta j)^2,$$

are the second derivatives, $d^2\varepsilon/d\eta^2$, in the cubic region. The latter do not need to be the same as those in the adjoining regions, but it is wise to keep them close to or at any rate bracketted by the values of the latter in order to prevent unnecessary variation of $d\varepsilon/d\eta$; this can be done by manually adjusting ε_1, ε_2, ε_1', ε_2', or Δj.

In the trivial case of an equal spacing in adjoining regions, the spacing in the transition zone will also be equal, provided that $\varepsilon_2 - \varepsilon_1 = \Delta j\ \Delta\phi_s$. With a uniform spacing of $\Delta\lambda_c$ on the grid sphere, the actual separation of points

TABLE I

Characteristics of Various Grids

Grid: (Fig.):	Spherical	**Asymm. bipolar (5)**	Madec & Imbard	Equatorial transform	**High lat. transition (8)**	**Conic section (10)**	**Inverse Goyou (11)**	**Multi-polar (13)**
Orthogonal	✓	✓	✓	✓	✓	✓	✓	✓
Smooth variation of grid size *along* grid lines	✓	✓	✓	jump	✓	✓	small jump[a]	✓
No singularities, small grid sizes, or strong convergence	No	✓	✓	✓	✓	✓	✓	✓
Grid compression at Equator	✓	No	✓	Possibly[b]	✓	Possibly[c]	✓	✓
Good resolution possible in Arctic	No[d]	With compress.	✓	No	✓	✓	✓	With compress.
Most of ocean on spherical grid (for coupling)	✓ (100%)	No	No	✓ (80%)	✓ (96%)	No	✓ (90%)	No
Bering Strait open(able)	✓	✓	✓	No	✓	✓	✓	✓
Single rectangular array	✓	✓	✓	No[e]	✓	✓	✓	✓

[a] May be possible to incorporate a smooth transition.
[b] Metric discontinuity at Equator would not disappear with compression.
[c] No metric discontinuities, but inexact alignment would require wider zone of compression.
[d] Compression possible, but cells would remain elongated and distorted near N. Pole.
[e] Not unless a curvilinear model were used.

in the bipolar region is given by differentiating the expression for the projection plane distance

$$\begin{aligned} a &= \tan[(90^\circ - \varepsilon)/2] \\ &= r_P \tan[(90^\circ - (\eta - j_2)\,\Delta\lambda_c)/2] \end{aligned} \tag{A3}$$

(see Fig. A1) w.r.t. η and rearranging, viz.,

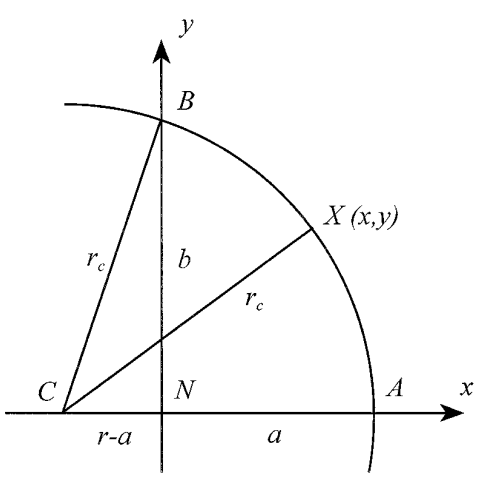

FIG. A1. Parameters associated with a *j*-circle passing through a point *X* in the transition zone.

$$d\varepsilon/d\eta = r_P \frac{1 + a^2/r_P^2}{1 + a^2}\,\Delta\lambda_c.$$

Step 2 is the placement of the *j*-lines in the transition region. The *j*-lines in the spherical domain are all concentric with the Pole; those of the bipolar grid and, hence, also those of the transition grid are not concentric with the Pole but are located at various points on the *x*-axis. From triangle *CNB* in Fig. A1, it will be seen that the radius of curvature, r_c, of a *j*-circle is related to the distances, *a* and *b*, from the Pole at which it crosses the *x* and *y* axes by

$$b^2 = a(2r_c - a).$$

It is convenient to use *a* as a parameter for the circular contours; this is related to ε by Eq. (A3). In the spherical region, the radius of a circle and its derivative w.r.t. *a* are just

$$r_c = a, \quad \frac{dr_c}{da} = 1.$$

The meridians of the bipolar grid all intersect the *y*-axis at $b = r_P$; the radius and its derivative in this case are, therefore,

$$r_c = \frac{a}{2} + \frac{r_P^2}{2a}, \quad \frac{dr_c}{da} = \frac{1}{2} + \frac{r_P^2}{2a^2}.$$

The cubic matching for $r_c = r_c(a)$ in terms of its value and derivative at $j = j_1, j_2$ are performed in the same way as for $\varepsilon(\eta)$. The function $r_c(a)$ for Fig. 8 is illustrated in Fig. A2.

Step 3 is the construction of the *i*-lines in the transition region. Orthogonal trajectories can be made from any non-overlapping set of contours, given certain assumptions about the variation of metric factors between grid lines. This is made possible by the fact that each circle is wholly determined by the parameter a, which is a function of ε and hence of η. A circle in the transition zone is described by the equation

$$y^2 = r_c^2 - x_c^2,$$

where $x_c = [x + (r_c - a)]$ is the x-component of XC. Partial differentiation w.r.t. a, with y and x separately being held constant, gives

$$\left.\frac{\partial x}{\partial a}\right|_y = \left[r_c \frac{dr_c}{da} - x_c\left(1 - \frac{dr_c}{da}\right)\right] \div x_c,$$
$$\left.\frac{\partial y}{\partial a}\right|_x = \left[r_c \frac{dr_c}{da} - x_c\left(1 - \frac{dr_c}{da}\right)\right] \div y. \tag{A4}$$

From a consideration of the geometry of the situation, the derivatives along *i*-lines are

$$\left.\frac{\partial x}{\partial a}\right|_\xi = \frac{x_c^2}{r_c^2}\left.\frac{\partial x}{\partial a}\right|_y, \quad \left.\frac{\partial y}{\partial a}\right|_\xi = \frac{y^2}{r_c^2}\left.\frac{\partial y}{\partial a}\right|_y. \tag{A5}$$

The *i*-lines may then be extended by integrating

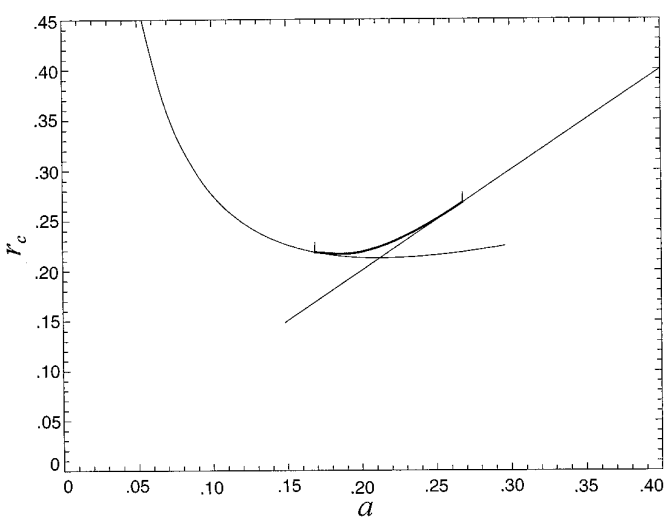

FIG. A2. Cubic matching of $r_c(a)$ in the transition zone (bold line) to the variation in the bipolar region (left) and the spherical region (right). Parameters are as used in the construction of Fig. 8.

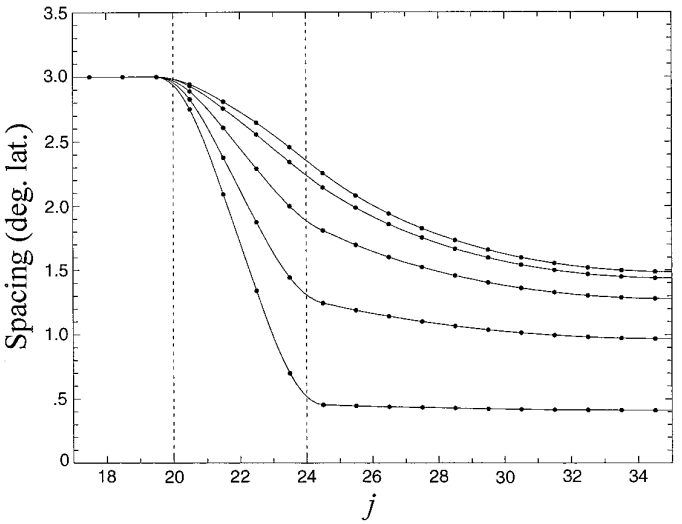

FIG. A3. Variation of grid-size along *i*-lines originating 0° (top), 20°, 40°, 60°, and 80° (bottom) from the symmetry meridian in Fig. 8. The vertical dashed lines delimit the transition zone.

$$\left(\left.\frac{\partial x}{\partial \eta}\right|_\xi, \left.\frac{\partial y}{\partial \eta}\right|_\xi\right) = \left(\left.\frac{\partial x}{\partial a}\right|_\xi, \left.\frac{\partial y}{\partial a}\right|_\xi\right)\frac{da}{d\varepsilon}\frac{d\varepsilon}{d\eta},$$

where $d\varepsilon/d\eta$ and $da/d\varepsilon$ are obtained by differentiating Eq. (A2) w.r.t. η and the first equality of Eq. (A3) w.r.t. η, viz.,

$$\frac{d\varepsilon}{d\eta} = \frac{\varepsilon_1 - \varepsilon_2}{\Delta j} + [(-3\delta^2 + 6\delta - 2)\varepsilon_1'' + (3\delta^3 - 1)\varepsilon_2'']\frac{\Delta j}{6}, \tag{A6}$$

$$\frac{da}{d\varepsilon} = -\frac{1}{2}\sec^2[(90° - \varepsilon)/2] = -\frac{1}{2}(1 + a^2). \tag{A7}$$

The values of r_c and a, required for evaluating Eqs. (A4), (A5), and (A7), are obtained by an iteration involving the relations

$$r_c = r_c(a), \quad x_c = \sqrt{r_c^2 - y^2}, \quad a = r_c + x - x_c.$$

For Eq. (A6), η is obtained by iteratively inverting Eq. (A2). The bipolar grid is constructed last because the latitudes of their parallels are not equally spaced but need to be determined for the intercepts of the projected *i*-lines at $j = j_2$ by inversion of Eqs. (A1) and (5).

Analytical expressions for the metric factors in the spherical and bipolar regions have been given by Eq. (7) and (8). In the transition region, the metric factor in the j direction is

$$\frac{\partial s}{\partial \eta} = \frac{1}{m}\left[\left(\frac{\partial x}{\partial \eta}\right)^{-2} + \left(\frac{\partial y}{\partial \eta}\right)^{-2}\right]^{1/2}$$
$$= \frac{1}{m}\left[\frac{dr_c}{da} - \frac{x_c}{r_c}\left(1 - \frac{dr_c}{da}\right)\right]\frac{da}{d\varepsilon}\frac{d\varepsilon}{d\eta},$$

where m is as defined in Eq. (13). The manner in which the changes in grid size have been spread over a number of grid rows is shown for several i-lines in Fig. A3. As the spacing of the grid points along j-rows is determined by the orthogonal trajectories, the metric coefficients $\partial s/\partial \xi$ would need to be calculated numerically.

ACKNOWLEDGMENTS

The author thanks Dr. A. C. Hirst, of the Division of Atmsopheric Research, Aspendale, Victoria, Australia, and Dr. I. Simmonds, of the University of Melbourne, for comments on the draft.

REFERENCES

1. A. F. Blumberg and G. L. Mellor, ''A Description of a Three-Dimensional Coastal Ocean Circulation Model,'' in *Three-Dimensional Coastal Ocean Models, Coastal Esturine Sci.*, Vol. 4, edited by N. Heaps (Amer. Geophys. Union, Washington, 1987).
2. G. L. Browning, J. J. Hack, and P. N. Swarztrauber, *Mon. Weather Rev.* **117,** 1058 (1989).
3. A. C. Coward, P. D. Killworth, and J. R. Blundell, *J. Geophys. Res.* **99,** 22725 (1994).
4. E. Deleersnijder, J-P. Van Ypersele, and J-M. Campin, *Ocean Modelling* **100,** 7 (1993).
5. M. Eby and G. Holloway, *Climate Dyn.* **10,** 241 (1994).
6. D. B. Haidvogel, J. L. Wilkin, and R. Young, *J. Comput. Phys.* **94,** 151 (1991).
7. K. S. Hedström, *User's Manual for a Semi-Spectral Primitive Equation Regional Ocean-Circulation Model Version 3.0* (Institute for Naval Oceanography, Stennis Space Center, 1992).
8. W. D. Hibler III and K. Bryan, *J. Phys. Oceanogr.* **17,** 987 (1987).
9. D. C. Ives and R. M. Zacharias, *Conformal Mapping and Orthogonal Grid Generation, AIAA/SAE/ASME/ASEE 23rd Joint Propulsion Conference, San Diego, 1987* (unpublished).
10. L. P. Lee, *Conformal Projections Based on Elliptic Functions* (Cartographica, Monograph No. 16, York University, Toronto; *Canad. Cartogr., Suppl.* **13** (1976).
11. G. Madec and M. Imbard, *Climate Dyn.*, **12,** in press (1996).
12. O. Marti, G. Madec, and P. Delecleuse, *J. Geophys. Res.* **97,** 12763 (1992).
13. J. M. Oberhuber, *J. Phys. Oceanogr.* **23,** 830 (1993).
14. M. Rančić, R. J. Purser, and F. Mesinger, *Quart. J. R. Meteor. Soc.*, **122,** in press (1996).
15. C. J. C. Reason and S. B. Power, *Climate Dyn.* **9,** 363 (1994).
16. A. J. Semtner Jr., *J. Phys. Oceanogr.* **6,** 409 (1976).
17. A. J. Semtner Jr., *J. Phys. Oceanogr.* **17,** 1077 (1987).
18. G. Starius, *Numer. Math.* **28,** 243 (1977).
19. J. F. Thompson, Z. U. A. Warsi, and C. W. Mastin, *J. Comput. Phys.* **47,** 1 (1982).
20. J. F. Thompson, Z. U. A. Warsi, and C. W. Mastin, *Numerical Grid Generation, Foundations and Applications* (North-Holland, Amsterdam, 1985).
21. J. L. Wilkin, 1987 (unpublished).
22. D. L. Williamson, ''Difference Appoximations for Fluid Flow on a Sphere,'' in *Numerical Methods used in Atmospheric Models*, Vol. 2, GARP Publ. Ser., No. 1, WMO-ICSU (GARP, Geneva, 1979).